Microscopy and Image Analysis

Microscopic analysis was carried out using a high-speed spinning disk confocal system (Ultraview ERS, Perkin Elmer) mounted on an inverted Axiovert 200 microscope (Carl Zeiss) with Optovar option linked to a Orca II ER camera (Hamamatsu, Japan). Image files were processed using ImageJ. Sporozoites in the dermis of mice were imaged as already described (Amino et al., 2007).

Primary Hepatocytes

Rat (4-week-old female Wistar) and mouse (6- to 8-week-old female C57BL/6) hepatocytes (Janvier, France) were isolated from animals treated with sodium pentobarbital by a modified two-step collagenase perfusion method. Briefly, the liver was perfused via the portal vein for 10 min with liver perfusion medium 1× (GIBCO 17701) followed by a 10 min perfusion with liver digest medium 1× (GIBCO 17703) at a flow rate of 6–10 ml/min. Isolated cells were washed and centrifuged through a Percoll gradient to remove damaged cells. Cell viability (>90%) was determined by trypan blue exclusion. Hepatocytes were plated at a density of 6–15 × 10^4 in 8-well permanox Lab-Tek chamber slides in Williams medium E containing 10% FCS. Cells were maintained at 37°C in a humidified atmosphere of 95% air and 5% CO_2.

Cell Traversal Assays

Cell traversal events by sporozoites were visualized by spinning disk confocal microscopy. Sporozoites and freshly trypsinized cells in a 1:1 ratio were mixed to 10 µl Matrigel (BD Biosciences) in the presence of 5 µM SYTOX Orange Nucleid Acid Stain (S-11368, Molecular Probes), a high-affinity nucleic acid stain that penetrates cells with a compromised plasma membrane. Samples were recorded for 30 min in multiple z layers with a double wavelength excitation of 488 nm and 568 nm for GFP-expressing parasites and SYTOX Orange, respectively.

Cell Infection Assays and CS Staining

Infection assays were performed at a multiplicity of infection of 1. Eight-well permanox Lab-Tek chamber slides and 15 × 10^4 sporozoites freshly dissected out from mosquito salivary glands were used in experiments with rat primary hepatocytes; MatTek glass bottom culture dishes and 2 × 10^4 sporozoites were used for CRL-2017 dermal fibroblasts infection. First, sporozoites were added onto cells on ice, and samples were centrifuged for 1 min at 4°C at 800 rpm to facilitate parasite-host cell interactions. Samples were then placed at 37°C, and at various incubation times samples were fixed with 4% paraformaldehyde (PFA), which does not permeabilize the host cell plasma membrane, and stained with the 3D11 anti-CS mAb coupled to Alexa Fluor 568 (A-20184, Molecular Probes). This allowed for discriminating between internalized sporozoites (green) and external sporozoites (red). Note that, in the case of the wild-type sporozoites, a proportion of the green parasites after 1 hr correspond to sporozoites that are located inside a cell, but not inside a vacuole (sporozoites arrested during cell traversal), a proportion that does not exceed 5%–10%.

Sporozoite Attachment Assay

Infection experiments were performed with 1.75 × 10^4 salivary gland sporozoites and a confluent monolayer of CRL-2017 dermal fibroblasts plated on Lab-Tek chamber slides (8-well permanox). Sporozoites were plated on cells in the presence of cytD 1 µg/ml, and after 15 min at 37°C, samples were washed three times in PBS and then stained with an Ab-CS to differentiate intracellular from extracellular parasites. As expected, no intracellular parasites were found. In experiments with metabolic inhibited parasites, sporozoites were preincubated 1 hr at room temperature with 0.03% sodium azide and then plated on cells in the continued presence of this compound.

Transmission Electron Microscopy

Samples were fixed by addition of 2.5% glutaraldehyde/0.15 M cacodylate buffer followed by 1% osmium tetroxyde, dehydrated in a series of ethanol concentrations, and embedded in EPON resin mixture. Ultrathin sections (50 to 60 nm) were observed with a Jeol 1200EXII (Tokio, Japon) transmission electron microscope. Images were recorded using an Eloise Keenview camera and the Analysis Pro software version 3.1 (Eloise SARL, Roissy, France).

Real-Time Quantitative RT-PCR

Real-time qPCR was performed on cDNA preparations using the SYBR green detection system and the ABI Prism 7900 sequence detector (Applied Biosystems) according to the manufacturer's instructions. Salivary gland sporozoites from the ConF, SpectF, and Spect2F clones were isolated at day 21 after the blood meal. RNA was extracted with TriZol and DNase treated, and cDNAs synthesized with Superscript II reverse transcriptase (Invitrogen) using random primers. Three independent RNA preparations were made for each sample. PCR conditions were 1 cycle of 95°C for 10 min followed by 40 cycles of 95°C for 15 s, 55°C for 15 s, and 60°C for 45 min). qPCR was performed in triplicate with three serial dilutions. The standard curve was analyzed for all primers and gave amplification efficiencies of 90%–100%. Data were analyzed with SDS 2.1 software. Analysis was performed using the $2^{-\Delta\Delta Ct}$ method (User Bulletin 2, ABI). The following primers were used for qPCR analysis: Ama1, forward, ATTTGGGTTGATGGTTATTG; Ama1, reverse, TCCTTGTCGAAATTTGGTAG; CS, forward, ACAGAGGAATGGTCTCAATG; CS, reverse, TTATCCATTTTACAAATTTCAG; TRAP, forward, AACATTCACTCCATTCTTCC; TRAP, reverse, CATGTTATTCCAATGCTCAC; P36p, forward, CTAATACGACCTTAGGACACTTTGAA; P36p, reverse, GATGTTCCATTTGGGTTTACATGATC; P36, forward, GCCTAATGCAAAATATTATCCCGATTTAG; P36, reverse, GCTAGTCCTTTGTTCCCATTATATG; Pbpl/UIS10, forward, GTTACACTGATAGAGAAGATGT; Pbpl/UIS10, reverse, GTGGTACTATACAAACAATATGTTGG; Spect2, forward, AAGGAGTTTCAGCTATGCAC; Spect2, reverse, CAGTTCATTTATGCCTGACC; Spect1, forward, TAGCCTAATTCAAATAAACGAAC; Spect1, reverse, GAAGTTAATTAATTCTGATACCCT; UIS4, forward, CCAAACCAAGCGATCATACATACAG; UIS4, reverse, CTTCACCCACTAAATCGCTTAATTC; S6, forward, GCTAGTGAAATCGAAGAAGC; S6, reverse, GCCTTGCAAATAATGAGAAC; Hsp70, forward, TGCAGCAGATAATCAAACTC; Hsp70, reverse, ACTTCAATTTGTGGAACACC; PbActin, forward, GGAAACATTATAACAGTAGGTAATGAAAG; PbActin, reverse, GTTGTACCTCCAGATAAAACAATGTTTCC; Tsrp, forward, TAAAGATAAGAGCACGAGTTAGTAGT; Tsrp, reverse, AATTGTTACATATTTACTTAGCATTCT; Celtos, forward, GTTCTATGTTTGAGAGGCAAAAATGG; Celtos, reverse, TGATGACGAGTCTTGTTGAAATGCAC; UIS3, forward, AGTTGCAATTGCTTTGTTATCATCAGGA; UIS3, reverse, GTTCTTTATATTTTGTACTAGTGCTTGGC.

Supplemental Data

The Supplemental Data include six supplemental figures and four supplemental movies and can be found with this article online at http://www.cellhostandmicrobe.com/cgi/content/full/3/2/88/DC1/.

ACKNOWLEDGMENTS

We thank S. Shorte, P. Roux, and the other members of the "Platforme d'imagerie dynamique" (Institut Pasteur) for help with confocal microscopy; C. Bourgouin, I. Thiéry, and the other members of the "Centre de Production et d'Infection des Anophèles" (Institut Pasteur) for mosquito rearing; V. Richard from the Electron Microscopy Facility (University of Montpellier 2); G. Milon, G. Lauvau, and T. Graf for providing the *lys-gfp* mice; and Patricia Baldacci and Samantha Blazquez for comments on the manuscript. This work was supported by funds from the Institut Pasteur ("Grand Programme Horizontal Anopheles"), the Howard Hughes Medical Institute, the European Commission (FP6 BioMalPar Network of Excellence), and the Core Research for Evolutional Science and Technology (CREST). R.A. was supported by the Pasteur Institute GPH fellowship, D.G. is a BioMalPar Ph.D. student, T.I. was supported by a fellowship from the Association Pasteur-Japon, M.Y. is a CREST Scholar, and R.M. is a Howard Hughes Medical Institute International Scholar.

Received: August 2, 2007
Revised: October 18, 2007
Accepted: December 26, 2007
Published: February 13, 2008

REFERENCES

Amino, R., Martin, B., Thiberge, S., Celli, S., Shorte, S., Frischknecht, F., and Ménard, R. (2006). Quantitative imaging of *Plasmodium* transmission from mosquito to mammal. Nat. Med. *12*, 220–224.

Amino, R., Thiberge, S., Blazquez, S., Baldacci, P., Renaud, O., Shorte, S., and Ménard, R. (2007). Imaging malaria sporozoites in the dermis of the mammalian host. Nat. Protocols *2*, 1705–1712.

Baer, K., Roosevelt, M., Clarkson, A.B., Jr., van Rooijen, N., Schnieder, T., and Frevert, U. (2007). Kupffer cells are obligatory for *Plasmodium yoelii* sporozoite infection of the liver. Cell. Microbiol. *9*, 397–412.

Bhanot, P., Schauer, K., Coppens, I., and Nussenzweig, V. (2005). A surface phospholipase is involved in the migration of *Plasmodium* sporozoites through cells. J. Biol. Chem. *280*, 6752–6760.

Carrolo, M., Giordano, S., Cabrita-Santos, L., Corso, S., Vigario, A.M., Silva, S., Leiriao, P., Carapau, D., Armas-Portela, R., Comoglio, P.M., et al. (2003). Hepatocyte growth factor and its receptor are required for malaria infection. Nat. Med. *9*, 1363–1369.

Coppi, A., Tewari, R., Bishop, J.R., Bennett, B.L., Lawrence, R., Esko, J.D., Billker, O., and Sinnis, P. (2007). Heparan sulfate proteoglycans provide a signal to *Plasmodium* sporozoites to stop migrating and productively invade host cells. Cell Host Microbe *2*, 316–327.

Courret, N., Darche, S., Sonigo, P., Milon, G., Buzoni-Gatel, D., and Tardieux, I. (2006). CD11c- and CD11b-expressing mouse leukocytes transport single *Toxoplasma gondii* tachyzoites to the brain. Blood *107*, 309–316.

Faust, N., Varas, F., Kelly, L.M., Heck, S., and Graf, T. (2000). Insertion of enhanced green fluorescent protein into the lysozyme gene creates mice with green fluorescent granulocytes and macrophages. Blood *96*, 719–726.

Frevert, U., Engelmann, S., Zougbede, S., Stange, J., Ng, B., Matuschewski, K., Liebes, L., and Yee, H. (2005). Intravital observation of *Plasmodium berghei* sporozoite infection of the liver. PLoS Biol. *3*, e192. 10.1371/journal.pbio.0030192.

Hollingdale, M.R., Leef, J.L., McCullough, M., and Beaudouin, R.L. (1981). *In vitro* cultivation of the exoerythrocytic stage of *Plasmodium berghei* from sporozoites. Science *213*, 1021–1022.

Ishino, T., Yano, K., Chinzei, Y., and Yuda, M. (2004). Cell-passage activity is required for the malarial parasite to cross the liver sinusoidal cell layer. PLoS Biol. *2*, 77–84.

Ishino, T., Chinzei, Y., and Yuda, M. (2005a). A *Plasmodium* sporozoite protein with a membrane attack complex domain is required for breaching the liver sinusoidal cell layer prior to hepatocyte infection. Cell. Microbiol. *7*, 199–208.

Ishino, T., Chinzei, Y., and Yuda, M. (2005b). Two proteins with 6-cys motifs are required for malarial parasites to commit to infection of the hepatocyte. Mol. Microbiol. *58*, 1264–1275.

Kaiser, K., Camargo, N., Coppens, I., Morrisey, J.M., Vaidya, A.B., and Kappe, S.H. (2004). A member of a conserved *Plasmodium* protein family with membrane-attack complex/perforin (MACPF)-like domains localizes to the micronemes of sporozoites. Mol. Biochem. Parasitol. *133*, 15–26.

Kappe, S.H., Buscaglia, C.A., and Nussenzweig, V. (2004). *Plasmodium* sporozoite molecular cell biology. Annu. Rev. Cell Dev. Biol. *20*, 29–59.

Kariu, T., Ishino, T., Yano, K., Chinzei, Y., and Yuda, M. (2006). CelTOS, a novel malarial protein that mediates transmission to mosquito and vertebrate hosts. Mol. Microbiol. *59*, 1369–1379.

Labaied, M., Camargo, N., and Kappe, S.H. (2007). Depletion of the *Plasmodium berghei* thrombospondin-related sporozoite protein reveals a role in host cell entry by sporozoites. Mol. Biochem. Parasitol. *153*, 158–166.

Lambert, H., Hitziger, N., Dellacasa, I., Svensson, M., and Barragan, A. (2006). Induction of dendritic cell migration upon *Toxoplasma gondii* infection potentiates parasite dissemination. Cell. Microbiol. *8*, 1611–1623.

Leiriao, P., Rodrigues, C.D., Albuquerque, S.S., and Mota, M.M. (2004). Survival of protozoan intracellular parasites in host cells. EMBO Rep. *5*, 1142–1147.

Matsuoka, H., Yoshida, S., Hirai, M., and Ishii, A. (2002). A rodent malaria, *Plasmodium berghei*, is experimentally transmitted to mice by merely probing of infective mosquito, *Anopheles stephensi*. Parasitol. Int. *51*, 17–23.

Ménard, R. (2001). Gliding motility and cell invasion by Apicomplexa: Insights from the *Plasmodium* sporozoite. Cell. Microbiol. *3*, 63–73.

Mota, M.M., Pradel, G., Vanderberg, J.P., Hafalla, J.C., Frevert, U., Nussenzweig, R.S., Nussenzweig, V., and Rodriguez, A. (2001). Migration of *Plasmodium* sporozoites through cells before infection. Science *291*, 141–144.

Mota, M.M., Hafalla, J.C.R., and Rodriguez, A. (2002). Migration through host cells activates *Plasmodium* sporozoites for infection. Nat. Med. *8*, 1318–1322.

Mota, M.M., and Rodriguez, A. (2004). Migration through host cells: The first steps of *Plasmodium* sporozoites in the mammalian host. Cell. Microbiol. *6*, 1113–1118.

Mueller, A.K., Camargo, N., Kaiser, K., Andorfer, C., Frevert, U., Matuschewski, K., and Kappe, S.H. (2005a). Plasmodium liver stage developmental arrest by depletion of a protein at the parasite-host interface. Proc. Natl. Acad. Sci. USA *102*, 3022–3027.

Mueller, A.K., Labaied, M., Kappe, S.H., and Matuschewski, K. (2005b). Genetically modified Plasmodium parasites as a protective experimental malaria vaccine. Nature *433*, 164–167.

Pimenta, P.F., Touray, M., and Miller, L. (1994). The journey of malaria sporozoites in the mosquito salivary gland. J. Eukaryot. Microbiol. *41*, 608–624.

Pradel, G., and Frevert, U. (2001). Malaria sporozoites actively enter and pass through rat Kupffer cells prior to hepatocyte invasion. Hepatology *33*, 1154–1165.

Prudencio, M., Rodriguez, A., and Mota, M.M. (2006). The silent path to thousands of merozoites: The *Plasmodium* liver stage. Nat. Rev. Microbiol. *11*, 849–856.

Sibley, L.D. (2004). Intracellular parasite invasion strategies. Science *304*, 248–253.

Sidjanski, S., and Vanderberg, J.P. (1997). Delayed migration of *Plasmodium* sporozoites from the mosquito bite site to the blood. Am. J. Trop. Med. Hyg. *57*, 426–429.

Silvie, O., Franetich, J.F., Charrin, S., Mueller, M.S., Siau, A., Bodescot, M., Rubinstein, E., Hannoun, L., Charoenvit, Y., Kocken, C.H., et al. (2004). A role for apical membrane antigen 1 during invasion of hepatocytes by Plasmodium falciparum sporozoites. J. Biol. Chem. *279*, 9490–9496.

Sinnis, P., Clavijo, P., Fenyo, D., Chait, B.T., Cerami, C., and Nussenzweig, V. (1994). Structural and functional properties of region II-plus of the malaria circumsporozoite protein. J. Exp. Med. *180*, 297–306.

Sturm, A., Amino, R., van de Sand, C., Regen, T., Retzlaff, S., Rennenberg, A., Krueger, A., Pollok, J.M., Ménard, R., and Heussler, V.T. (2006). Manipulation of host hepatocytes by the malaria parasite for delivery into liver sinusoids. Science *313*, 1287–1290.

Sultan, A.A., Thathy, V., Frevert, U., Robson, K.J., Crisanti, A., Nussenzweig, V., Nussenzweig, R., and Ménard, R. (1997). TRAP is necessary for gliding motility and infectivity of *Plasmodium* sporozoites. Cell *90*, 511–522.

Vanderberg, J.P., Chew, S., and Stewart, M.J. (1990). *Plasmodium* sporozoite interactions with macrophages *in vitro*: A videomicroscopic analysis. J. Protozool. *37*, 528–536.

Vanderberg, J.P., and Frevert, U. (2004). Intravital microscopy demonstrating antibody-mediated immobilisation of *Plasmodium berghei* sporozoites injected into skin by mosquitoes. Int. J. Parasitol. *34*, 991–996.

van Dijk, M.R., Douradinha, B., Franke-Fayard, B., Heussler, V., van Dooren, M.W., van Schaijk, B., van Gemert, G.J., Sauerwein, R.W., Mota, M.M., Waters, A.P., and Janse, C.J. (2005). Genetically attenuated, P36p-deficient malarial sporozoites induce protective immunity and apoptosis of infected liver cells. Proc. Natl. Acad. Sci. USA *102*, 12194–12199.

van Rooijen, N., Bakker, J., and Sanders, A. (1997). Transient suppression of macrophage functions by liposome-encapsulated drugs. Trends Biotechnol. *15*, 178–185.

Waters, A.P., Mota, M.M., van Dijk, M.R., and Janse, C.J. (2005). Parasitology. Malaria vaccines: Back to the future? Science *307*, 528–530.

Yamauchi, L.M., Coppi, A., Snounou, G., and Sinnis, P. (2007). *Plasmodium* sporozoites trickle out of the injection site. Cell. Microbiol. *9*, 1215–1222.

Molecular Microbiology (2009) 71(6), 1402–1414 ■

doi:10.1111/j.1365-2958.2009.06609.x
First published online 11 February 2009

Identification of a transcription factor in the mosquito-invasive stage of malaria parasites

Masao Yuda,[1]* Shiroh Iwanaga,[2] Shuji Shigenobu,[3] Gunnar R. Mair,[4] Chris J. Janse,[4] Andrew P. Waters,[5] Tomomi Kato[1] and Izumi Kaneko[1]

[1]*Department of Medical Zoology, Mie University School of Medicine, Mie, Tsu, 514-0001, Japan.*
[2]*Department of Medical Zoology, Tottori University School of Medicine, Tottori, Yonago, Japan.*
[3]*Okazaki Institute for Integrative Bioscience, National Institute for Basic Biology, National Institutes of Natural Sciences, Higashiyama, Myodaiji, Okazaki, Japan.*
[4]*Department of Parasitology, Leiden University Medical Centre, 2333 ZA Leiden, the Netherlands.*
[5]*University of Glasgow, Glasgow Biomedical Research Centre, Glasgow, Scotland, UK.*

Summary

Gene expression in *Plasmodium* parasites undergoes significant changes in each developmental stage, but the transcription factors (TFs) regulating these changes have not been identified. We report here a *Plasmodium* TF (AP2-O) that activates gene expression in ookinetes, the mosquito-invasive form, and has a DNA-binding domain structurally related to that of a plant TF, Apetala2 (AP2). AP2-O mRNA is presynthesized by intraerythrocytic female gametocytes and translated later during ookinete development in the mosquito. The *Plasmodium* TF activates a set of genes, including all genes reported to be required for midgut invasion, by binding to specific six-base sequences on the proximal promoter. These results indicate that AP2 family TFs have important roles in stage-specific gene regulation in *Plasmodium* parasites.

Introduction

Elucidation of gene regulation mechanisms in the parasitic protozoan *Plasmodium* could provide important information for understanding parasite developmental programmes and its interactions with both host and vector during infection at each infection stage and could support the development of new antimalarial strategies. However, at present, little is known about the mechanisms of gene regulation in *Plasmodium* and only a small number of transcription factors (TFs), which may bind to specific DNA promoter sequences and control gene expression, have been predicted in the *Plasmodium* genome (Iyer *et al.*, 2008).

At present the Apetala2 (AP2) family is the only known gene family predicted to encode TF candidates in the *Plasmodium* genome (Balaji *et al.*, 2005). The AP2 family TFs were first identified in plants (Jofuku *et al.*, 1994) and then shown to form a large family in the genome of several plants (Gutterson and Reuber, 2004). In *Arabidopsis thaliana*, the AP2 family contains at least 140 members, some of which are involved in stress responses and others in regulation of reproductive and vegetative organ development (Gutterson and Reuber, 2004). Plant AP2 family TFs are named for their possession of at least one common DNA-binding domain of approximately 60 amino acids, the AP2 domain. A bioinformatic analysis of the complete *Plasmodium falciparum* genome revealed that AP2-related genes are present in apicomplexan genomes, including *Plasmodium* (Balaji *et al.*, 2005), where in the human malaria parasite *Plasmodium falciparum*, 26 AP2-related genes were predicted. The predicted *Plasmodium* AP2-related genes encode proteins with one to four AP2 domains; however, their function remains to be elucidated.

Plasmodium has three host-invasive stages: merozoites, ookinetes and sporozoites, which are erythrocyte-, mosquito midgut- and salivary gland/Kuppfer cell/hepatocyte-invasive stages respectively. These stages produce various stage-specific proteins involved in subsequent host invasion, some of which have been identified through various transcriptome and proteome analyses (Kaiser *et al.*, 2004; Hall *et al.*, 2005; Raibaud *et al.*, 2006). Each invasive form of the parasite produces a distinct repertoire of proteins that are secreted from apical secretory organelles such as micronemes and rhoptries and associated with invasion of host cells or tissues (Dubremetz *et al.*, 1998) or associated with the cell surface, suggesting that they participate in specific host–parasite interactions. However, regulatory mechanisms of individual or groups of stage-specific genes remain elusive in all these stages.

Accepted 12 January, 2009. *For correspondence. E-mail m-yuda@doc.medic.mie-u.ac.jp; Tel. (+81) 59 231 5430; Fax (+81) 59 231 5430.

During asexual replication in animal host erythrocytes, some *Plasmodium* parasites differentiate into sexual forms, called gametocytes. When ingested by a mosquito with a blood meal, gametocytes generate gametes that are fertilized and form zygotes in the mosquito midgut lumen. The zygotes develop into motile ookinetes that invade the midgut epithelium and differentiate into oocysts on the basal side of the midgut. The developing ookinetes produce large amount of stage-specific proteins for subsequent midgut invasion (Vlachou *et al.*, 2006) including microneme proteins such as circumsporozoite protein thrombospondin-related anonymous protein (TRAP)-related protein (CTRP), a protein belonging to the TRAP family and essential for gliding motility (Dessens *et al.*, 1999; Yuda *et al.*, 1999a); chitinase, a chitinolytic enzyme necessary for ookinete crossing of the mosquito chitin-containing peritrophic matrix (Vinetz *et al.*, 2000); membrane attack ookinete protein (MAOP), essential for rupture of mosquito midgut epithelial cell membrane (Kadota *et al.*, 2004); a protein kinase CDPK3 (calcium-dependant protein kinase 3) that stimulates invasion (Ishino *et al.*, 2006); cell surface-associated proteins, P28 and P25, which are necessary for ookinete development and are transmission-blocking vaccine targets (Tomas *et al.*, 2001; Saul, 2007); and other secreted proteins (Yuda *et al.*, 2001; Dessens *et al.*, 2003). The expression of some ookinete-specific proteins is regulated at the translational level where the female *Plasmodium* gametocyte represses specific transcripts through a protein complex composed of DOZI (development of zygotes inhibited), a conserved DDX6-class RNA helicase, and other proteins (Mair *et al.*, 2006). After fertilization, these gene transcripts are released from the complex and enter the translation pathway. On the other hand, *de novo* mRNA synthesis of invasion-related genes also occurs after fertilization (Raibaud *et al.*, 2006), and full-scale production of invasion-related proteins begins several hours after fertilization in developing ookinetes.

During a systematic investigation of the predicted AP2 factors that are not expressed in asexual blood-stage parasites we discovered one we designate AP2-O (AP2 in ookinetes) that is essential for the formation of invasive ookinetes and the expression of ookinete invasion-related genes. Here, we report that AP2-O is the ookinete TF that directly activates the invasion-related genes by binding to a specific motif found upstream of them.

Results

Expression of AP2-O *is regulated at translational level*

Plasmodium berghei AP2-O (PB000572.01.0) encodes a protein with a single AP2 domain and has an orthologue in *P. falciparum* (PF11_0442, Fig. 1A) and other *Plasmodium* spp. AP2-O has two conserved regions which include the AP2 domain near the C-terminus. The amino acid sequences of the AP2-O AP2 domain are almost identical among *Plasmodium* spp. (Fig. S1).

To investigate *AP2-O* protein expression, a transgenic line of *P. berghei* that expressed green fluorescent protein (GFP) fused to the endogenous allele of *AP2-O* (AP2-O::GFP parasites) was generated (Fig. 1B). The fusion did not appear to affect the parasite's ability to infect mosquitoes, as the AP2-O::GFP parasite generated a normal number of oocysts in mosquitoes (Table 1). In the blood stages of AP2-O::GFP parasites, fluorescence of the GFP-fused protein was not observed (Fig. 1C). However, weak fluorescent signals were observed in retort-form ookinetes beginning 8 h after fertilization (Fig. 1C). The signals were localized in the nucleus and signal intensities increased with ookinete development.

We also compared the amount of *AP2-O* transcripts between gametocytes and ookinetes with real-time reverse transcription PCR (RT-PCR) analysis using wild-type (WT) asexual-free parasite preparations (Fig. 1D). Unexpectedly the analysis showed that *AP2-O* transcripts are most abundant in the gametocyte stage and markedly decreased in the subsequent zygote and ookinete stages. This expression profile was in contrast with that of the typical ookinete microneme protein, secreted ookinete adhesive protein (SOAP), whose transcripts are mainly synthesized in the zygote and ookinete stages (Dessens *et al.*, 2003). These results suggest that *AP2-O* expression is translationally repressed in female gametocytes and subsequently translated in ookinetes (Mair *et al.*, 2006).

We examined whether *AP2-O* transcripts form physical complexes with DOZI in gametocytes using immunoprecipitation (IP) experiments on DOZI::GFP gametocytes (Fig. 1E). *AP2-O* transcripts were co-precipitated with GFP-tagged DOZI with anti-GFP antibodies. These results demonstrated that the translation repression system of the DOZI complex controls expression of AP2-O mRNA.

AP2-O *disruption decreases expression of several mosquito invasion-related genes*

To investigate the function of *AP2-O*, we prepared *P. berghei* mutant parasites with the *AP2-O*-disrupted [*AP2-O* (–)] (Fig. 2A). The *AP2-O* (–) parasites formed morphologically normal female and male gametocytes and exhibited normal exflagellation rates (Table 1). However, they lacked the ability to infect mosquitoes as no oocysts or sporozoites were found in the mosquito midgut. In culture, *AP2-O* (–) parasites formed zygotes at normal conversion rates and differentiated into retort forms by 9 h after fertilization, as in WT parasites (Fig. 2B, top). Subtle morphological differences between WT and

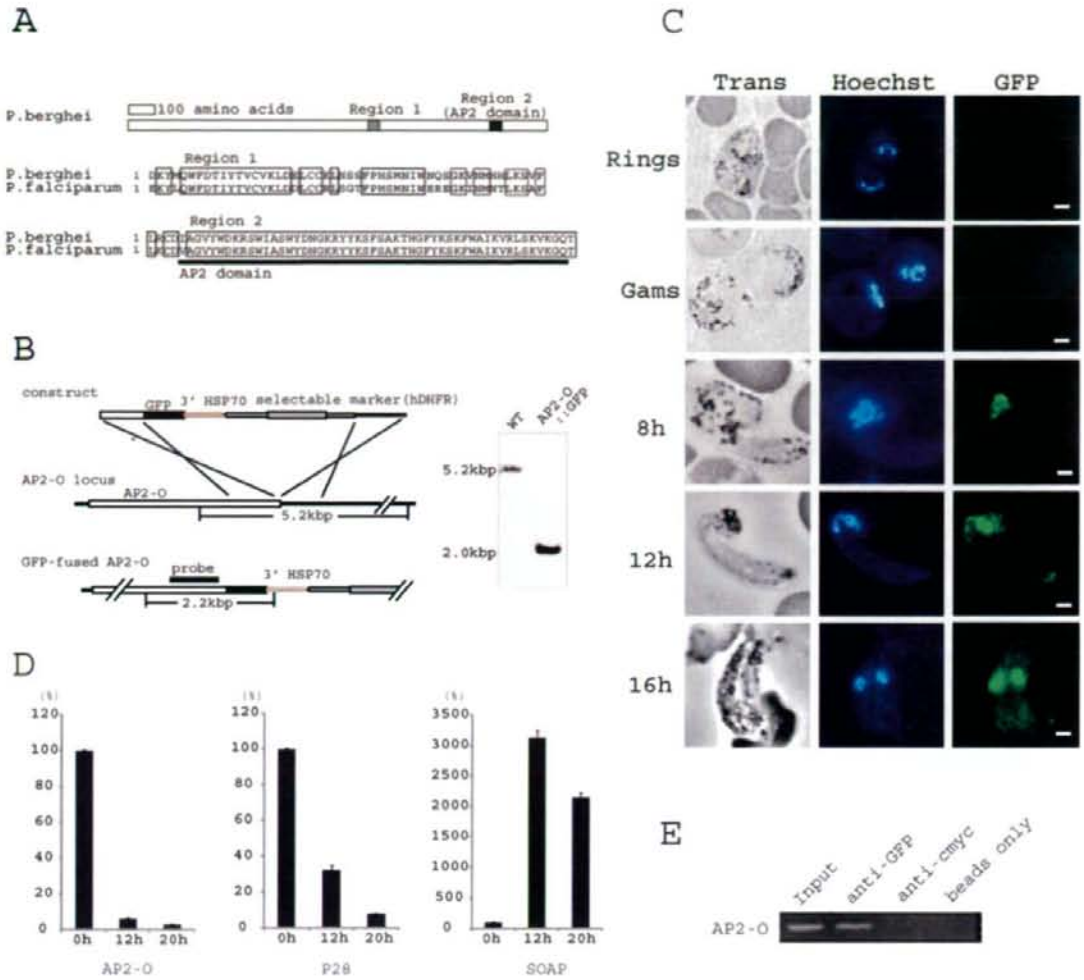

Fig. 1. Expression of AP2-O is controlled at the translational level.

A. The amino acid sequences around the single AP2 domain and another conserved region (region 1) were aligned between *Plasmodium berghei* and *P. falciparum*. Identical amino acids are highlighted by rectangles.

B. To construct AP2-O::GFP parasites, the targeting vector containing a marker gene (left top), human DHFR (hDHFR), was integrated into the *AP2-O* locus (left middle) by double-cross-over recombination, adding the GFP gene to the C-terminal portion of *AP2-O* and conferring pyrimethamine resistance to the AP2-O::GFP parasites (left bottom). For Southern hybridization (right), WT and AP2-O::GFP genomic DNA was digested with MunI and hybridized with a probe (solid bar; bottom left). Integration decreased detected fragment size from 5.2 to 2.0 kb.

C. To localize AP2-O *in vivo*, AP2-O::GFP parasites were cultured to the ookinete stage. At 8, 12 and 16 h after fertilization, nuclei were stained with Hoechst 34580. Images of blood-stage parasites were also shown. Rings, ring forms; Gams, gametocytes. Scale bars, 2 μm.

D. Total RNA was prepared from asexual-free blood-stage parasites (0 h), retort-form ookinetes (12 h after fertilization) and mature ookinetes (20 h after fertilization) cultured from the same infected blood. Quantitative RT-PCR was performed with primers for *AP2-O*, *P28* and *SOAP*. Each result is the mean of three independent experiments with standard error bars. For each gene, the amount of mRNA at each time was expressed as the per cent of mRNA relative to that at 0 h after fertilization. P28 mRNA is abundant in gametocytes, while SOAP mRNA is mainly synthesized in ookinetes. *AP2-O* showed an expression pattern different from that of *SOAP*.

E. For analysis of complex formation of *AP2-O* mRNA and the translation repression complex, IP was performed on gametocyte lysate of DOZI::GFP parasites using anti-GFP antibodies, anti-myc antibodies and protein G Sepharose beads only. RNAs recovered from IPs were analysed by RT-PCR with primers for *AP2-O*.

Table 1. *AP2* (–) malaria parasites lack the ability to infect mosquitoes.[a]

Genotype	Exflagellation rate	Conversion rate[b]	Number of oocysts per mosquito[c]	Number of sporozoites per mosquito[d]
WT	44.6	63.8 (6.8)	76.1 (14.73)	40 604 (6957)
AP2 (–) 1	37.5	56.8 (11.9)	0	0
AP2 (–) 2	24.3	71.0 (2.3)	0	0
AP2-O::GFP	35	70.5 (1.12)	71.6 (20.85)	42 940 (6797)

a. Infected mice were subjected to mosquito bites when exflagellation rates became more than 20 per 10^5 red blood cells. Fully engorged mosquitoes were dissected after 14 days, and the numbers of oocysts and sporozoites in the midgut were counted.
b. Conversion rates (%) of female gametocytes to retort-form ookinetes (standard errors in parentheses).
c. Twenty mosquitoes were dissected, and the number per mosquito was calculated (standard errors in parentheses).
d. Ten mosquitoes were dissected, and the number per mosquito was calculated (standard errors in parentheses).

AP2-O (–) parasites, however, became visible 12 h after fertilization with a swelling protrusion in the retort forms (Fig. 2B, centre). Final development was aberrant ookinetes with an pear-shaped form, different from the sword-like form of WT ookinetes (Fig. 2B, bottom).

Cross-fertilization experiments mating *AP2-O* (–) mutant gametocytes with those from either female or male gametocyte-defective lines indicated that the *AP2-O* defect is inherited from the female line (Fig. 2C). *AP2-O* (–) females when fertilized with WT males produced deformed ookinetes. However, WT females when fertilized by *AP2-O* (–) males produced normal ookinetes. These results suggest that *AP2-O* transcripts in zygotes/ookinetes are derived from female gametocytes and essential for zygote development into normal infective ookinetes.

DNA microarray analyses were performed to investigate whether *AP2-O* disruption affects gene expression in ookinetes. Samples were obtained from WT and *AP2-O* (–) retort-form ookinetes at 12 h after fertilization, when slight morphological differences between them started to appear (Fig. 2B, centre). Genes were selected whose expression was decreased at least fivefold (Fig. 2D). A total of 15 genes were identified with this analysis, of which four were ookinete-specific genes (all encoding microneme proteins) (Yuda *et al.*, 1999b; 2001; Vinetz *et al.*, 2000; Dessens *et al.*, 2003), six were genes reported to be transcribed during ookinete development after zygote formation (Raibaud *et al.*, 2006) and five were novel genes not ascribed to. We performed real-time RT-PCR analysis in the five novel genes and showed that they were transcribed in the zygote/ookinete stage (Fig. S2). Very recently two of them (PB000652.03.0 and PB001214.00.0) were reported to be involved in ookinete midgut invasion (Ecker *et al.*, 2008). As shown in Table S1 and Fig. 2D, 14 of these 15 proteins have orthologous genes in *P. falciparum* and *P. vivax*, and 10 have a putative N-terminal signal peptide sequence, suggesting that they are microneme or cell surface-associated proteins that are available for subsequent midgut invasion.

AP2-O directly activates several genes by binding to a six-base sequence, TAGCTA

To investigate which of the 15 genes AP2-O regulates directly, chromatin immunoprecipitation (ChIP) assays were performed on AP2-O::GFP parasites (Fig. 3A and Fig. S3). The upstream promoter region of all genes was significantly enriched by ChIP with anti-GFP antibody. Enrichment was not observed in identical assays performed on WT parasites. These results indicated that AP2-O regulates all 15 genes directly and that there is at least one binding site for AP2-O in the upstream region of each gene. Therefore, we looked for putative AP2-O binding sites in these 15 genes by determining high-frequency sequences in the 1 kb immediate upstream regions of these genes using a computational analysis (Table S2). The sequence conservation pattern (Fig. 3B) shows a 6 bp sequence, TAGCTA, as the most frequently occurring sequence. This sequence was present in the upstream region of 14 of the 15 genes, with two or more TAGCTA sequences observed in 13 genes (Fig. 3C). In addition to TAGCTA, four other closely related sequences, TGGCTA/TAGCCA and CAGCTA/TAGCTG, are possible binding sites for AP2-O (see Fig. 3E). Including the less frequent binding elements, TGGCTA/TAGCCA, two or more binding sites were present in all 15 genes. Frequencies of CAGCTA/TAGCTG were significantly low compared with the other three binding sequences (Table S2). The majority of the binding sequences were adjacent (approximately 100–400 bp upstream) to the putative transcription start site as estimated from the most upstream expressed sequence tags (ESTs) of each gene (Fig. 3C).

Electrophoretic mobility shift assays (EMSA) were performed to examine whether the 6 bp sequences act as binding sites for AP2-O. The ~300 bp *SOAP* upstream region, which contains two TAGCTA sites, was used as the probe (Fig. 3D). The AP2 domain of AP2-O bound to the probe and produced a single band shift. Addition of a point mutation (TAGCTA to TAGGTA) in one of the two TAGCTA sites significantly reduced the intensity of the

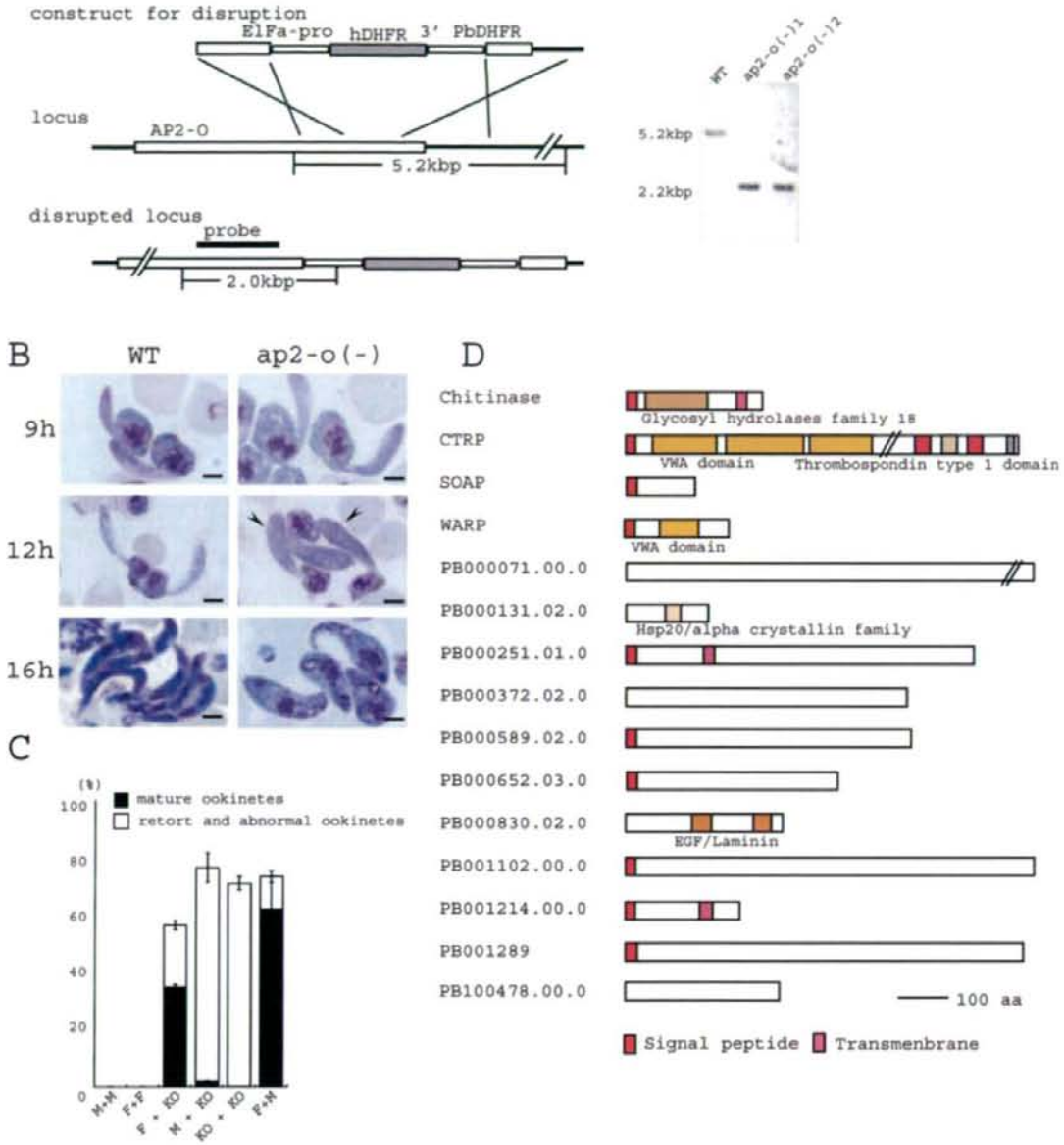

shifted band, and addition of the mutation in both sites eliminated the band shift. The same results were obtained using the ~300 bp upstream region of the chitinase gene (Fig. S4A).

To further analyse the binding specificity of the AP2 domain, we performed EMSA using probes with various point mutations in the TAGCTA sequence. Of the 18 mutations examined, 14 nearly eliminated binding and 4 (TGGCTA/TAGCCA and CAGCTA/TAGCTG) moderately reduced band shift intensity (Fig. 3E). These results demonstrated that AP2-O preferentially binds to TAGCTA, but also binds with weaker affinity to the similar sequences.

Fig. 2. AP2-O is necessary for normal development of ookinetes and expression of invasion-related genes.
A. To construct *AP2-O* (–) parasites, a targeting vector (left top) containing a selectable marker gene was integrated into the *AP2-O* locus (left middle) by double-cross-over recombination resulting in disruption of the *AP2-O* gene and conferring pyrimethamine resistance to the *AP2-O* (–) mutants (left bottom). For Southern hybridization (right), WT and *AP2-O* (–) genomic DNA was digested with MunI and hybridized with a probe (solid bar; left bottom). Integration decreased fragment size from 5.2 to 2.2 kb. Independently prepared *AP2-O* (–) mutants, *AP2-O* (–) 1 and *AP2-O* (–) 2, exhibited the same phenotype.
B. Phenotype of *AP2-O* (–) parasites in Giemsa-stained cultured ookinetes at different times after fertilization. A morphological difference between WT and *AP2-O* (–) parasites apparent 12 h after fertilization was the swelling protrusion (arrowheads) in *AP2-O* (–) retort-form ookinetes. *AP2-O* (–) parasites developed into pear-shaped ookinetes 16 h after fertilization (lower right). Scale bars, 2 μm.
C. Cross-fertilization experiments were performed with *AP2-O* (–) parasites, a male-deficient line (*P48/45*$^-$) and a female-deficient line (*P47*$^-$). Conversion rates of female gametocytes to deformed ookinetes and mature normal ookinetes are shown. The abnormal ookinetes observed in the combination of *AP2-O* (–) mutants and a male-defective line (*P48/45*$^-$) may have derived from self-fertilization of *AP2-O* (–) mutants. M, female-deficient line (*P47*$^-$); F, a male-deficient line (P48/45$^-$); KO, *AP2-O* (–) parasites.
D. Names or IDs of 15 *P. berghei* genes whose expression was decreased at least fivefold in *AP2-O* (–) ookinetes compared with WT (left), and the structure of their encoded proteins (right).

TAGCTA as a cis*-acting element in the ookinete stage*

Reporter assays were carried out to investigate whether the TAGCTA sequence functions as a *cis*-acting element *in vivo*. For these assays a plasmid containing a *P. berghei* centromere was used (Fig. S4B). This plasmid acts as an artificial chromosome and is maintained stably through several cell divisions in transfected parasites (S. Iwanaga *et al.*, unpubl. results). The upstream region of the SOAP gene, containing three TAGCTA sequences, was inserted upstream of the GFP reporter gene, and *P. berghei* blood-stage parasites were transfected with this construct (Fig. 4). GFP signals were not observed in the intraerythrocytic stages, including gametocytes. In ookinete cultures, GFP signals were detected 8 h after fertilization and signal intensity increased with ookinete development (data not shown), indicating that the upstream region acts as a stage-specific promoter. When one of the three TAGCTA sequences was disrupted by addition of a point mutation (TAGCTA to TAGGTA), promoter activity reduced to 40% of that of the non-mutated sequence; mutations in two of the TAGCTA sequences reduced promoter activity to < 10% of the non-mutated sequences. Similar results were obtained with the ~300 bp upstream region of the chitinase gene (Fig. S4C). These results indicate that the TAGCTA sequence functions as a *cis*-acting element *in vivo* and that the number of elements is an important factor in determining promoter activity.

cis*-acting elements are conserved among* Plasmodium *spp.*

The amino acid sequence of AP2 domain of AP2-O is highly conserved among several *Plasmodium* spp. (Fig. S1). Conservation of the amino acid sequence in the AP2 domain suggests that sequences recognized by this domain would be conserved among *Plasmodium* spp., and thus the same *cis*-acting elements would be observed in the orthologues of the 15 genes. To examine this, we performed computational analysis on *P. falciparum* and *P. vivax* orthologues (Tables S3 and S4, and Fig. 5A; 14 orthologues were used because orthologues of one *P. berghei* gene, PB100478.00, were not found in *P. falciparum* and *P. vivax*). In all three parasites, TAGCTA was conserved as the most frequently occurring sequence. The great majority of the *P. falciparum* and *P. vivax* orthologues had binding sequences for AP2-O in the upstream promoter region (11 of 14 and 13 of 14 respectively; Fig. 5B). Distribution of the binding sequences on each upstream region was also conserved among orthologues.

AP2-O activates all reported ookinete stage-specific genes

We analysed 15 genes whose expression significantly decreased in *AP2-O* (–) mutants. However, other genes, demonstrated or suggested to be involved in midgut invasion, *P25*, *P28*, *CDPK* and *MAOP* (Tomas *et al.*, 2001; Kadota *et al.*, 2004; Ishino *et al.*, 2006), were not in that initial group. To investigate whether these genes are regulated by AP2-O in the ookinete stage, we performed ChIP assays (Fig. 6A). The results demonstrated that AP2-O is associated with the upstream region in each of the four genes. Furthermore, two or more AP2-O binding sites were identified in the upstream region of each gene (Fig. 6B). These results indicate that these genes are activated by AP2-O in the ookinete stage.

Discussion

Global surveys of gene expression indicated that a high proportion of *Plasmodium* genes are expressed in a stage-specific manner (Le Roch *et al.*, 2003). However, how these changes are regulated in the life cycle remains elusive. In this study, we showed that specific gene expression in the ookinete stage is regulated by a sequence-specific TF belonging to the AP2 family, AP2-O. This study provided the first experimental evidence that gene expression in plasmodium is regulated by specific TF.

Ookinetes express several genes necessary for midgut invasion during development in mosquito midgut lumen.

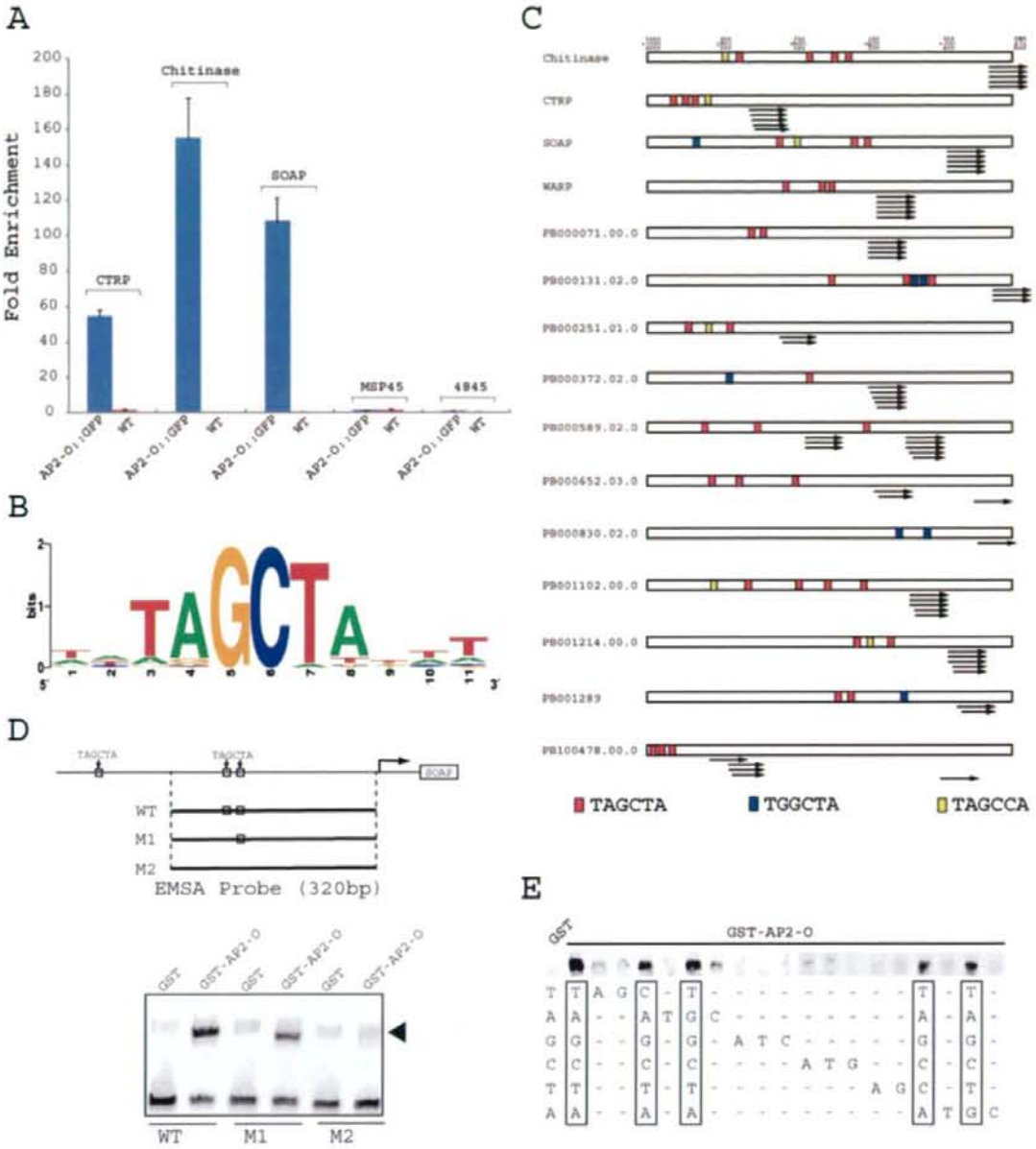

Gene expression begins at 8–10 h after fertilization and continues for approximately 10 h until midgut invasion starts (Yuda *et al.*, 1999b; 2001). Our results showed that AP2-O is expressed during this period and activates several genes by directly binding to their upstream region. The activated genes encode different types of proteins including secretory proteins, surface-associated proteins and cytoplasmic proteins and include all known ookinete-specific genes involved in midgut invasion. Therefore, AP2-O would be a master activator that induces a cluster of different genes necessary for midgut invasion.

Our reporter assays indicated that the number of binding sites for AP2-O on the upstream promoter may be a factor defining promoter activities in the ookinete stage.

Fig. 3. AP2-O binds specifically to six-base sequences on the proximal promoter region of ookinete stage-specific genes.
A. For analysis of AP2-O complexes with the genes in Fig. 2D, ChIP was performed in AP2-O::GFP ookinetes. Of the 15 genes listed in Fig. 2D, the results for *CTRP*, chitinase and *SOAP* and for the negative controls, *P48/45* and *MSP4/5*, which are not expressed in ookinetes, are shown. Values are fold enrichments relative to IPs with control antibodies. Control experiments with wild-type parasites (WT) were also performed. Three biologically independent ChIP experiments were performed, and essentially the same results were obtained. The results of one of these experiments were shown here. Each result is the mean of three independent quantitative PCR experiments with standard error bars. The results for several other *Plasmodium* spp. genes are shown in Fig. S2.
B. WebLogo diagram of sequences occurring at high frequency in the 1 kb upstream regions of the *P. berghei* genes listed in Fig. 2D. Graphical representations created by WebLogo (Crooks *et al.*, 2004).
C. AP2-O binding sequences and the furthest upstream five 5′-ESTs (arrows) in the 1 kb upstream regions of the *P. berghei* genes listed in Fig. 2D. In each gene, more than two AP2-O binding sequences are present 100–400 bp upstream from the most upstream EST cluster. Coloured rectangles indicate binding sequence locations.
D. Sequence specificity of AP2-O binding was detected by EMSA using a GST-fused AP2-O AP2 domain. The *SOAP* upstream region containing two TAGCTA sequences was used as the probe. Probes with one (M1) or two (M2) mutations in their TAGCTA sequence (TAGCTA to TAGGTA) were also used. TAGCTA sequences in the upstream region of WT (no mutation) and the two mutations are illustrated (top). GST was used as a negative control. In the EMSA gel (bottom), the arrowhead indicates the band shift.
E. Other sequence possibilities in the AP2 domain binding site. Various point mutations were added to the TAGCTA sequence, and binding to AP2-O was determined by EMSA. The added point mutations are indicated under each lane. Binding ability was lost or greatly reduced in most mutated probes. Those mutations retaining binding activity are highlighted by a rectangle.

The AP2-O binding sites are mainly located within a short 100–400 bp region from the transcription start site (Fig. 3C), suggesting that to activate target genes, AP2-O must bind to the region just upstream of the transcription initiation site.

The merozoite and sporozoite stages also produce large amounts of invasion-related proteins during the development to mature invasive forms. Our results suggest that AP2 family TFs regulate invasion-related genes in these stages of *Plasmodium* spp. In fact, this possibility is supported by some preceding studies. For example, in the asexual blood stages, genes for erythrocyte invasion are mainly expressed in the mid- to late-schizont stage, i.e. the stage preceding merozoites (Bozdech *et al.*, 2003). The expressed genes encode proteins necessary for erythrocyte invasion such as microneme and rhoptry proteins as well as several surface-associated proteins. Because at this period some AP2 family genes exhibit peak expression, these AP2 family genes might be TFs inducing these invasion-related genes (Balaji *et al.*, 2005). Recent study showed that one of such AP2-related protein binds to a specific sequence and that many invasion-related genes have this motif in the upstream (De Silva *et al.*, 2008), suggesting that the AP2-related gene encodes an activator of these genes. Although this suggestion should be tested further, it is compatible with our present finding that an AP2-related protein directly controls stage-specific expression of multiple genes in ookinetes. Also in sporozoites, several invasion-related genes are expressed and some of them are homologous to genes regulated by AP2-O (Yuda and Ishino, 2004). A recent *in silico* analysis reported that sporozoite-specific genes have a common six-base motif CATGCA in the upstream (Young *et al.*, 2008). Therefore, it is possible that this motif is a binding sequence for another activator belonging to the AP2 family. It remains for further study to explore which AP2 family genes are expressed during the formation of infective sporozoites.

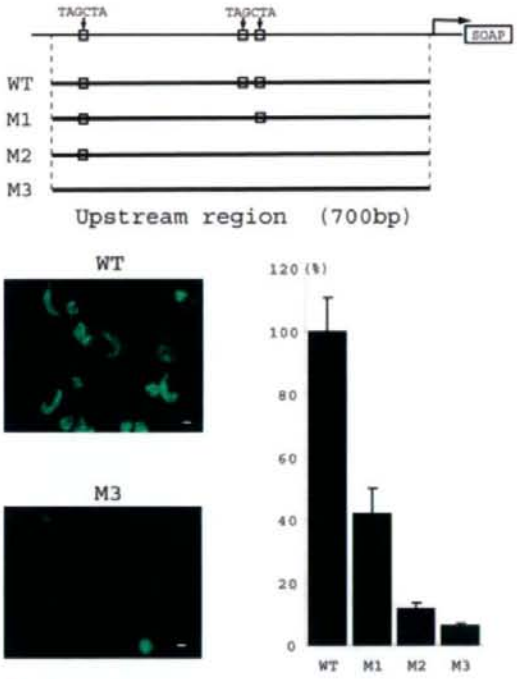

Fig. 4. The TAGCTA sequence as a *cis*-acting element in the ookinete stage. Promoter activity of the TAGCTA sequence in the ookinete stage *in vivo* was analysed using a reporter system with the *P. berghei* centromere plasmid Pcen (see also Fig. S3B). Mutations were added to three TAGCTA motifs in the SOAP upstream region (top). Mutations in M1 and M2 are the same as in M1 and M2 in Fig. 3D. M3 contains mutations in all three TAGCTA sequences. Each result is the mean of three independent experiments with standard error bars and is shown as the activity relative to that of the non-mutated WT. Representative images of GFP expression in ookinetes transfected with WT and M3 Pcen are shown at the bottom left. Round cells with strong fluorescence are mouse reticulocytes. Scale bars, 2 μm.

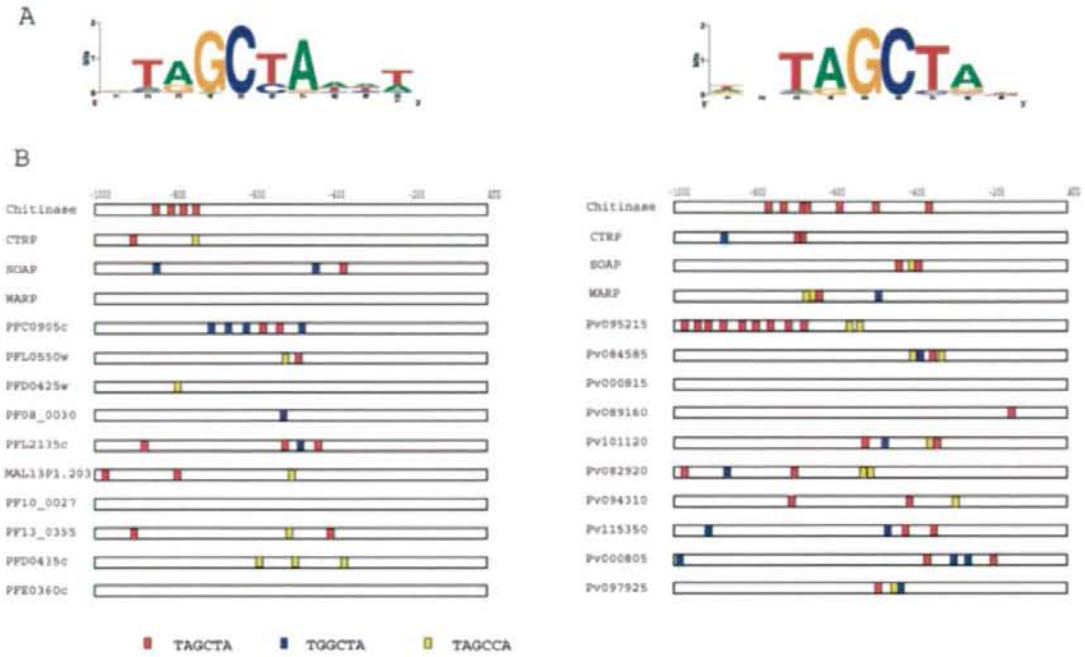

Fig. 5. Binding sequences for *Plasmodium berghei* AP2-O are conserved in *P. falciparum* and *P. vivax*.
A. WebLogo diagrams of sequences occurring at high frequency in the 1 kb upstream regions of the 14 orthologues in Fig. 2D in *P. falciparum* (left) and *P. vivax* (right). Graphical representations created by WebLogo (Crooks *et al.*, 2004).
B. AP2-O binding sequences in the 1 kb upstream regions of the 14 orthologues in Fig. 2D in *P. falciparum* (left) and *P. vivax* (right). Coloured rectangles indicate binding sequence locations.

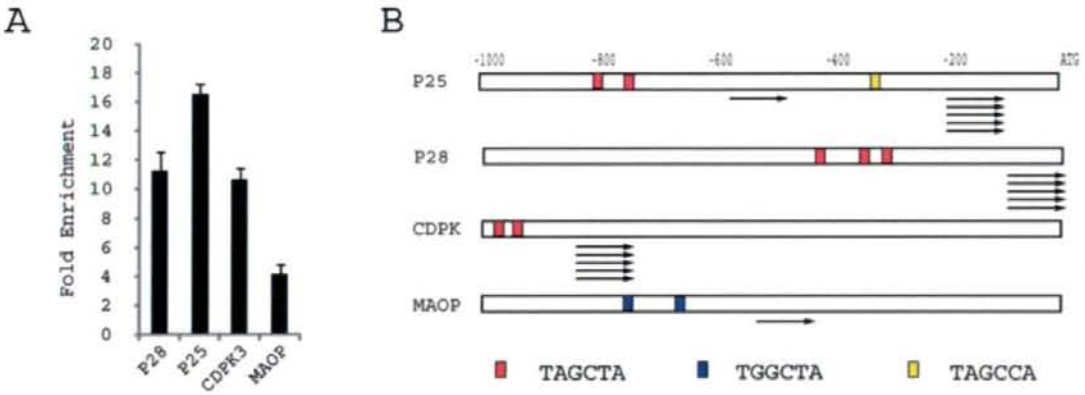

Fig. 6. Four *P. berghei* genes involved in ookinete invasion that are regulated by AP2-O.
A. ChIP was performed in *P28*, *P25*, *CDPK3* and *MAOP*, and DNA fragments were subjected to quantitative PCR with primers for upstream regions of the respective genes. Values are fold enrichments relative to IPs with control antibodies. Each result is the mean of three independent experiments with standard error bars.
B. AP2-O binding sequences and the most upstream 5′-ESTs (arrows) in the 1 kb upstream regions of four *P. berghei* genes are shown here. Each gene had more than two AP2-O binding sequences present 100–300 bp upstream from the most upstream EST cluster. Coloured rectangles indicate binding sequence locations.

In this study, genes regulated by AP2-O were first screened by comparison of gene expression between WT and *AP2-O* (–) parasites, and 15 genes were identified as being directly regulated by AP2-O. However, four genes reported so far were difficult to identify with this screening method. Of these genes, *P25* and *P28* were transcribed abundantly in female gametocytes (Paton *et al.*, 1993). Therefore, it seems that for these genes abundant transcripts had been synthesized in female gametocytes and masked the defect of transcription due to *AP2-O* disruption later in the ookinete stage. If so, many genes regulated by this TF could still remain to be identified.

In conclusion, our results demonstrate an AP2-related protein as a *Plasmodium* TF. At present, the *Plasmodium* AP2 family is the sole lineage-specific TF in *Plasmodium* spp. (Iyer *et al.*, 2008). Therefore, it is possible that these AP2 TFs participate in stage-specific gene regulations of *Plasmodium* spp. through their life cycle. Thus far, 26 AP2-related genes have been identified in the *Plasmodium* genome, but their roles in the life cycle, except for *AP2-O*, remain undefined. Further studies on AP2-related TFs are necessary to elucidate gene regulation mechanisms of *Plasmodium* parasites.

Experimental procedures

Parasite preparations

Female BALB/c mice infected (6–10 weeks old, Japan SLC, Hamamatsu, Japan) were prepared by peritoneal injection of *P. berghei* ANKA strain-infected blood that had been stored at –70°C. For ookinete culture, stored infected blood was injected intraperitoneally into mice that were made anaemic by phenyl-hydrazine treatment. After checking parasite exflagellation, infected blood was collected from the mice, passed through a CF11 column to deplete WBC, and diluted 10-fold with pH 8.0 RPMI1600 medium (Gibco, Gaithersburg, MD, USA), pH 8.0, containing 20% fetal calf serum and penicillin/streptomycin, and incubated at 20°C for 20–24 h. To prepare asexual-free gametocytes and ookinetes, infected anaemic mice were treated for 2 days with sulphadiazine (Sigma, St Louis, MO, USA) in their drinking water (10 μg ml^{-1}) to kill asexual stage parasites. Parasite infectivity in mosquitoes was evaluated as follows. When exflagellation rates were increased to over $20/10^5$ red blood cells, infected mice were subjected to bites of *Anopheles stephensi* mosquitoes. Fully engorged mosquitoes were selected and maintained at 20°C. After 2 week, the mosquitoes were dissected and the numbers of oocysts and sporozoites in their midguts were counted.

Cross-fertilization experiments

Cross-fertilization experiments were performed using a similar procedure to that described by Khan *et al.* (2005). *AP2-O* (–) parasites were fertilized with lines that have either defective male gametes (*P48/45*$^-$) or defective female gametes (*P47*$^-$). The numbers of unfertilized female gametes, deformed ookinetes and mature normal ookinetes were counted 20 h after fertilization, and conversion rates from female gametocytes to deformed ookinetes and mature normal ookinetes were calculated.

Genomic Southern hybridization

A 2 μg sample of *P. berghei* genomic DNA was digested with restriction enzymes, separated on a 1.5% agarose gel and transferred onto a nylon membrane. DNA fragments for Southern hybridization probes were amplified by PCR using genomic DNA as a template. The PCR primer pairs for AP2-O disruption were 5′-GCTGGAACTCCTTATTATGTTGCC-3′ and 5′-GCTTCAATCCACTATTTTCCAAACC-3′, and for the GFP-fused AP2-O-expressing mutants, the primers were 5′-GCTGGAACTCCTTATTATGTTGCC-3′ and 5′-GCT TCAATCCACTATTTTCCAAACC-3′. Amplified DNAs were labelled with alkaline phosphatase using AlkPhos Direct Labelling Reagents (Amersham Bioscience, Piscataway, NJ, USA) and subsequently detected using a CDP-Star chemiluminescent detection reagent (Amersham Bioscience).

Electrophoretic mobility shift assays (EMSA)

The *P. berghei* TF AP2 domain (amino acid residues 488–554) was produced as a glutathione S-transferase fusion protein using the GST Gene Fusion System with a pGEX 6p-1 vector (Amersham Bioscience). The AP2 domain coding region was amplified from *P. berghei* genomic DNA with the primer set: 5′-CGGGATCCGCCTTTAGGGTATTTGATGTAG AC-3′ and 5′-CCGCTCGAGTTAATACTTTAGTTTCATCATTT CGC-3′. The recombinant protein was purified with a glutathione Sepharose column (Amersham Bioscience). Longer probes were prepared by PCR with 5′-biotinylated primers using the cloned promoter region of *chitinase* or *SOAP* as templates. The primer pairs used were 5′-GGAGAGTTTT ATATTTTCAATTTTTATACTTAAAC-3′ and 5′-GAAAACGAA AAAAAGACAAATAAAAGAAC-3′ for *SOAP*, and 5′-ATTATT AATCACTATTTTATGGATGTAC-3′ and 5′-CCAAAAAATGG TGATATAGAAAAAGGC-3′ for the chitinase gene. Probes with a mutation in the TAGCTA sequence (TAGCTA to TAGGTA) were generated by PCR-mediated site-directed mutagenesis. Short oligonucleotide probes were prepared as follows. A synthetic 5′-biotinylated oligonucleotide was annealed with a complementary oligonucleotide to generate a double-strand probe. The oligonucleotide sequence was 5′-GTACATATTTTTTTGAATAGCTACCTTATTTTCCTTTGG-3′. Probes with various point mutations in the TAGCTA sequence were also prepared. EMSA was performed using a LightShift Chemiluminescence EMSA Kit (Pierce, Rockford, IL, USA). Briefly, GST-tagged protein (45 μg ml^{-1} final concentration) or GST as a control (30 μg ml^{-1} final concentration) was pre-incubated with a probe in EMSA buffer containing 50 ng μl^{-1} poly(dI-dC) for 20 min at room temperature. Gel electrophoresis was performed according to the manufacturer's protocol.

Targeted disruption of the AP2-O *gene*

The targeting vector was prepared by PCR according to Ecker *et al.* (2006). In brief, two fragments of the *AP2-O* gene were amplified by PCR using genomic DNA as the template with the primer pairs 5′-CGCGAGCTCGCAATATGGTATTA AATTTTGGGCTAGCCA-3′ (primer 1) and 5′-CGCGGATCC

GGTATTTTCATTGTGTTAAACGATATGTGA-3′ (primer 2), and 5′-CCGCTCGAGGTCCTATTTATCATTTTAAAATGTGT TTTATC-3′ (primer 3) and 5′-CGGGGTACCAATCGTCATA AATAGGAGTTATGAAGT-3′ (primer 4). The fragments were annealed to either side of the selectable marker gene (human DHFR) by PCR with primers 1 and 4. Gene targeting was performed as described previously (Yuda *et al.*, 1999a).

ChIP-quantitative PCR assays

ChIP was performed using a Chromatin Immunoprecipitation Assay Kit (Upstate Biotechnology, Lake Placid, NY, USA) according to the manufacturer's protocol. In brief, BALB/c mice (Japan SLC) were infected with malaria parasites expressing GFP-fused AP2-O (or WT parasites as a negative control) and treated with sulphadiazine to kill the parasite asexual stages. Blood was harvested and cultured to obtain ookinetes. After 20 h, each culture was fixed with 1% paraformaldehyde for 20 min at 30°C, washed with cold PBS, and incubated two or three times with NH_4Cl on ice for 30 min to lyse the erythrocytes. The ookinete-containing samples were sonicated in 250 μl of the lysis solution with a Bioruptor (Cosmo Bio, Tokyo, Japan) 10 times with a 30 s pulse and a 30 s interval. DNA fragmentation was checked by electrophoresis. IP was performed with anti-GFP polyclonal antibody (Clontech, Palo Alto, CA, USA) and pre-immune rabbit serum (negative control). DNA fragments obtained by IP were analysed by Real Time PCR using an iCycler iQ Real-Time Detection System (Bio-Rad, Hercules, CA, USA) with the primers listed in Table S5. Data were also presented as per cent input in Table S6.

Reporter assays with P. berghei *centromere plasmids*

Reporter assays were performed with the *P. berghei* centromere plasmid, Pcen (Fig. S3B). The upstream promoter region of the chitinase or SOAP gene (600 bp) was inserted into the EcoRV/BamHI site upstream of the GFP gene. This construct was transfected into cultured *P. berghei* shizonts by electroporation. Transfected parasites were selected by pyrimethamine to obtain parasites with the reporter construct. Ookinetes were cultured as described above and images were obtained with a fluorescent microscope equipped with a digital CCD camera system (Nikon, Kawasaki, Japan). Total fluorescent signal from each ookinete was analysed with Aqua Cosmos software (Hamamatsu Photonics, Hamamatsu, Japan). Background correction was performed by subtracting the intensity of a nearby cell-free region from the signal of the ookinete. Total of 30 ookinetes were used to determine promoter activity in each assay.

Construction of GFP-fused AP2-O-expressing parasites

GFP-fused AP2-O-expressing parasites (AP2-O::GFP) were constructed as follows. The targeted insertion vector was constructed in a pBluescript plasmid (Stratagene, La Jolla, CA, USA) (Fig. 1B). For the targeted insertion construct, a DNA fragment containing the 3′ part of the AP2-O coding region was amplified by PCR and inserted into the pBluescript XhoI/NheI site in frame with the GFP gene. The downstream region of the AP2-O gene was also amplified by PCR and inserted into the pBluescript BamHI/NotI site. Plasmids containing the construct were separated from plasmids without the construct by digestion with XhoI and NotI. AP2-O::GFP parasites were obtained by inserting the construct into the *AP2-O* locus by homologous recombination. Finally, AP2-O::GFP parasites were separated from WT by limiting dilution. GFP-fused protein fluorescence was observed with a microscope equipped with a filter set for GFP. For nuclear staining, Hoechst 34580 (Molecular Probes, Eugene, OR, USA) (0.02 μg ml^{-1} final concentration) was added to the medium, and the culture was incubated at room temperature for 10 min before fluorescence microscopy.

DNA microarray analysis

A custom 60-mer microarray (Agilent Technologies, Palo Alto, CA, USA) was designed based on *P. berghei* EST contigs (assembled from approximately 1×10^5 ESTs from different developmental stages, including blood stages, ookinetes, midgut sporozoites, salivary gland sporozoites and exoerythrocytic forms) and *P. berghei* genes in the NCBI Reference Sequence (RefSeq) Database (Pruitt *et al.*, 2007). This microarray contained approximately 21 000 probes and covered most *P. berghei* genes. Total RNA was prepared from malaria parasite blood stages and 12 h cultured ookinetes using RNAgents (Promega, Madison, WI, USA). Before RNA extraction, erythrocytes were lysed in 0.83% NH_4Cl. An RNA probe for one-colour analysis was synthesized using a Low RNA Fluorescent Linear Amplification Kit (Agilent Technologies) and fragmentated using a Gene Expression Hybridization Kit (Agilent Technologies) according to manufacturer's protocols. Hybridization was performed at 65°C. Three biologically independent experiments were performed in both *AP2-O* (–) and WT parasites. The data were analysed with Genespring software (Agilent Technologies). The data were normalized as follows. First, signal intensities less than 0.01 were set to 0.01. Then each chip was normalized to the 60th percentile of the measurements taken from the chip. Genes with significant differences between WT and *AP2-O* disruptants were selected by Student's *t*-test using *P*-value cut-off 0.05 (False discovery rate) and those whose expression was decreased at least fivefold in *AP2-O* (–) parasites were selected as candidates regulated by AP2-O. From the selected genes, those belonging to multigene families and those whose upstream sequences were not present in the *P. berghei* genome database were excluded. We have deposited the microarray data to Gene Expression Omnibus (GEO) DataSets with the Accession No. GSM359409–GSM359412, GSM359415 and GSM359428.

Quantitative RT-PCR

Quantitative analysis of *P. berghei AP2-O* expression was performed by quantitative RT-PCR. In brief, total RNA was extracted from asexual-free gametocytes and ookinetes. RT (1 μg of total RNA) was performed with random primers and Superscript II Reverse Transcriptase (Gibco BRL, Gaithersburg, MD, USA). SYBR Green PCR amplifications were performed using an iCycler iQ Real-Time Detection System (Bio-Rad Corporation) with the primer set: 5′-TTGGATT GCATCATGGTATG-3′ and 5′-TTCGGGGTTATTATTTTTAG GTTTTC-3′.

Identification of frequently occurring sequences in promoter regions

The frequency of occurrence of all possible 6 bp sequences in a gene's 1 kb upstream region was compared for the 15 genes in Fig. 2C and all annotated genes in the *P. berghei* genome (Table S2). Three 6 bp sequences, which had the five-base sequence TAGCT in common, were identified with significantly high frequencies (false discovery rate < 0.05) in the former group, and 10 of the 14 sequences with the highest frequency (false discovery rate < 0.5) could be aligned so that at least continuous 3 bp sequences overlap with each other. Based on the aligned sequences, the sequence conservation pattern in the 1 kb upstream regions of the 15 genes was generated using the fuzznuc and WebLogo programs (Olson, 2002; Crooks *et al.*, 2004).

Accession numbers

The PlasmoDB (http://www.plasmodb.org/plasmo/) accession number for *P. berghei AP2-O* is PB000572.01.0 and for *P. falciparum AP2-O* is PF11_0442. The reference numbers of blood-stage, ookinete and sporozoite ESTs are DC218765–DC224499, BB970378–BB981955, DC224500–DC235-241 respectively.

Acknowledgements

We thank N. Kimura for maintaining mosquito colonies. This work was supported by Ministry of Education, Science, Culture, and Sports of Japan (Grant 19041031, 19659105 and 20249023 to M.Y., and Grant 19041048 and 19790307 to S.I.). The research in the Leiden Malaria Research Group was supported by BioMalPar (EU).

References

Balaji, S., Babu, M.M., Iyer, L.M., and Aravind, L. (2005) Discovery of the principal specific transcription factors of Apicomplexa and their implication for the evolution of the AP2-integrase DNA binding domains. *Nucleic Acids Res* **33:** 3994–4006.

Bozdech, Z., Llinas, M., Pulliam, B.L., Wong, E.D., Zhu, J., and DeRisi, J.L. (2003) The transcriptome of the intraerythrocytic developmental cycle of *Plasmodium falciparum*. *PLoS Biol* **1:** E5.

Crooks, G.E., Hon, G., Chandonia, J.M., and Brenner, S.E. (2004) WebLogo: a sequence logo generator. *Genome Res* **14:** 1188–1190.

De Silva, E.K., Gehrke, A.R., Olszewski, K., Leon, I., Chahal, J.S., Bulyk, M.L., and Llinas, M. (2008) Specific DNA-binding by apicomplexan AP2 transcription factors. *Proc Natl Acad Sci USA* **105:** 8393–8398.

Dessens, J.T., Beetsma, A.L., Dimopoulos, G., Wengelnik, K., Crisanti, A., Kafatos, F.C., and Sinden, R.E. (1999) CTRP is essential for mosquito infection by malaria ookinetes. *EMBO J* **18:** 6221–6227.

Dessens, J.T., Siden-Kiamos, I., Mendoza, J., Mahairaki, V., Khater, E., Vlachou, D., *et al.* (2003) SOAP, a novel malaria ookinete protein involved in mosquito midgut invasion and oocyst development. *Mol Microbiol* **49:** 319–329.

Dubremetz, J.F., Garcia-Reguet, N., Conseil, V., and Fourmaux, M.N. (1998) Apical organelles and host-cell invasion by Apicomplexa. *Int J Parasitol* **28:** 1007–1013.

Ecker, A., Moon, R., Sinden, R.E., and Billker, O. (2006) Generation of gene targeting constructs for *Plasmodium berghei* by a PCR-based method amenable to high throughput applications. *Mol Biochem Parasitol* **145:** 265–268.

Ecker, A., Bushell, E.S., Tewari, R., and Sinden, R.E. (2008) Reverse genetics screen identifies six proteins important for malaria development in the mosquito. *Mol Microbiol* **70:** 209–220.

Gutterson, N., and Reuber, T.L. (2004) Regulation of disease resistance pathways by AP2/ERF transcription factors. *Curr Opin Plant Biol* **7:** 465–471.

Hall, N., Karras, M., Raine, J.D., Carlton, J.M., Kooij, T.W., Berriman, M., *et al.* (2005) A comprehensive survey of the *Plasmodium* life cycle by genomic, transcriptomic, and proteomic analyses. *Science (New York)* **307:** 82–86.

Ishino, T., Orito, Y., Chinzei, Y., and Yuda, M. (2006) A calcium-dependent protein kinase regulates *Plasmodium* ookinete access to the midgut epithelial cell. *Mol Microbiol* **59:** 1175–1184.

Iyer, L.M., Anantharaman, V., Wolf, M.Y., and Aravind, L. (2008) Comparative genomics of transcription factors and chromatin proteins in parasitic protists and other eukaryotes. *Int J Parasitol* **38:** 1–31.

Jofuku, K.D., den Boer, B.G., Van Montagu, M., and Okamuro, J.K. (1994) Control of *Arabidopsis* flower and seed development by the homeotic gene APETALA2. *Plant Cell* **6:** 1211–1225.

Kadota, K., Ishino, T., Matsuyama, T., Chinzei, Y., and Yuda, M. (2004) Essential role of membrane-attack protein in malarial transmission to mosquito host. *Proc Natl Acad Sci USA* **101:** 16310–16315.

Kaiser, K., Matuschewski, K., Camargo, N., Ross, J., and Kappe, S.H. (2004) Differential transcriptome profiling identifies *Plasmodium* genes encoding pre-erythrocytic stage-specific proteins. *Mol Microbiol* **51:** 1221–1232.

Khan, S.M., Franke-Fayard, B., Mair, G.R., Lasonder, E., Janse, C.J., Mann, M., and Waters, A.P. (2005) Proteome analysis of separated male and female gametocytes reveals novel sex-specific *Plasmodium* biology. *Cell* **121:** 675–687.

Le Roch, K.G., Zhou, Y., Blair, P.L., Grainger, M., Moch, J.K., Haynes, J.D., *et al.* (2003) Discovery of gene function by expression profiling of the malaria parasite life cycle. *Science (New York)* **301:** 1503–1508.

Mair, G.R., Braks, J.A., Garver, L.S., Wiegant, J.C., Hall, N., Dirks, R.W., *et al.* (2006) Regulation of sexual development of *Plasmodium* by translational repression. *Science (New York)* **313:** 667–669.

Olson, S.A. (2002) EMBOSS opens up sequence analysis. European Molecular Biology Open Software Suite. *Brief Bioinform* **3:** 87–91.

Paton, M.G., Barker, G.C., Matsuoka, H., Ramesar, J., Janse, C.J., Waters, A.P., and Sinden, R.E. (1993) Structure and expression of a post-transcriptionally regulated malaria gene encoding a surface protein from the sexual stages of *Plasmodium berghei*. *Mol Biochem Parasitol* **59:** 263–275.

Pruitt, K.D., Tatusova, T., and Maglott, D.R. (2007) NCBI

reference sequences (RefSeq): a curated non-redundant sequence database of genomes, transcripts and proteins. *Nucleic Acids Res* **35:** D61–D65.

Raibaud, A., Brahimi, K., Roth, C.W., Brey, P.T., and Faust, D.M. (2006) Differential gene expression in the ookinete stage of the malaria parasite *Plasmodium berghei*. *Mol Biochem Parasitol* **150:** 107–113.

Saul, A. (2007) Mosquito stage, transmission blocking vaccines for malaria. *Curr Opin Infect Dis* **20:** 476–481.

Tomas, A.M., Margos, G., Dimopoulos, G., van Lin, L.H., de Koning-Ward, T.F., Sinha, R., *et al.* (2001) P25 and P28 proteins of the malaria ookinete surface have multiple and partially redundant functions. *EMBO J* **20:** 3975–3983.

Vinetz, J.M., Valenzuela, J.G., Specht, C.A., Aravind, L., Langer, R.C., Ribeiro, J.M., and Kaslow, D.C. (2000) Chitinases of the avian malaria parasite *Plasmodium gallinaceum*, a class of enzymes necessary for parasite invasion of the mosquito midgut. *J Biol Chem* **275:** 10331–10341.

Vlachou, D., Schlegelmilch, T., Runn, E., Mendes, A., and Kafatos, F.C. (2006) The developmental migration of *Plasmodium* in mosquitoes. *Curr Opin Genet Dev* **16:** 384–391.

Young, J.A., Johnson, J.R., Benner, C., Yan, S.F., Chen, K., Le Roch, K.G., *et al.* (2008) In silico discovery of transcription regulatory elements in Plasmodium falciparum. *BMC Genomics* **9:** 70.

Yuda, M., and Ishino, T. (2004) Liver invasion by malarial parasites – how do malarial parasites break through the host barrier? *Cell Microbiol* **6:** 1119–1125.

Yuda, M., Sakaida, H., and Chinzei, Y. (1999a) Targeted disruption of the plasmodium berghei CTRP gene reveals its essential role in malaria infection of the vector mosquito. *J Exp Med* **190:** 1711–1716.

Yuda, M., Sawai, T., and Chinzei, Y. (1999b) Structure and expression of an adhesive protein-like molecule of mosquito invasive-stage malarial parasite. *J Exp Med* **189:** 1947–1952.

Yuda, M., Yano, K., Tsuboi, T., Torii, M., and Chinzei, Y. (2001) von Willebrand Factor A domain-related protein, a novel microneme protein of the malaria ookinete highly conserved throughout *Plasmodium* parasites. *Mol Biochem Parasitol* **116:** 65–72.

Supporting information

Additional supporting information may be found in the online version of this article.

Please note: Wiley-Blackwell are not responsible for the content or functionality of any supporting materials supplied by the authors. Any queries (other than missing material) should be directed to the corresponding author for the article.

Malaria-Specific and Nonspecific Activation of CD8$^+$ T Cells during Blood Stage of *Plasmodium berghei* Infection[1]

Mana Miyakoda,* Daisuke Kimura,* Masao Yuda,‡ Yasuo Chinzei,‡ Yoshisada Shibata,† Kiri Honma,* and Katsuyuki Yui[2]*

Cerebral malaria is one of the severe complications of *Plasmodium falciparum* infection. Studies using a rodent model of *Plasmodium berghei* ANKA infection established that CD8$^+$ T cells are involved in the pathogenesis of cerebral malaria. However, it is unclear whether and how *Plasmodium*-specific CD8$^+$ T cells can be activated during the erythrocyte stage of malaria infection. We generated recombinant *Plasmodium berghei* ANKA expressing OVA (OVA-PbA) to investigate the parasite-specific T cell responses during malaria infection. Using this model system, we demonstrate two types of CD8$^+$ T cell activations during the infection with malaria parasite. Ag (OVA)-specific CD8$^+$ T cells were activated by TAP-dependent cross-presentation during infection with OVA-PbA leading to their expression of an activation phenotype and granzyme B and the development to functional CTL. These highly activated CD8$^+$ T cells were preferentially sequestered in the brain, although it was unclear whether these cells were involved in the pathogenesis of cerebral malaria. Activation of OVA-specific CD8$^+$ T cells in RAG2 knockout TCR-transgenic mice during infection with OVA-PbA did not have a protective role but rather was pathogenic to the host as shown by their higher parasitemia and earlier death when compared with RAG2 knockout mice. The OVA-specific CD8$^+$ T cells, however, were also activated during infection with wild-type parasites in an Ag-nonspecific manner, although the levels of activation were much lower. This nonspecific activation occurred in a TAP-independent manner, appeared to require NK cells, and was not by itself pathogenic to the host. ***The Journal of Immunology*, 2008, 181: 1420–1428.**

Malaria remains one of the crucial threats to public health in much of the world. It has been well accepted that Ab and CD4$^+$ T cells play critical roles for protection against malaria parasites that can be acquired during natural or experimental infection (1–4). However, the role of CD8$^+$ T cells in protective immunity is controversial. Some studies suggested that CD8$^+$ T cells could transfer protective immunity to an adoptive host (5), whereas others claimed that they did not play a major role in protection against blood stage infection with *Plasmodium* species (6). In contrast, accumulating evidence indicates that CD8$^+$ T cells are involved in the pathogenesis of severe malaria. Cerebral malaria resulting from *Plasmodium falciparum* infection is one of the most severe complications and main cause of death in human malaria (7–11). Using a rodent model of malaria infection with the *Plasmodium berghei* ANKA (PbA)[3] strain, investigations indicated that CD8$^+$ T cells are one of the major effector cells that trigger cerebral malaria. In these experimental models, it was shown that CD8$^+$ T cells were sequestered in the brain during cerebral malaria and that the depletion of CD8$^+$ T cells decreased mortality (8). Furthermore, perforin-mediated killing by CD8$^+$ T cells was required for the pathogenesis of experimental cerebral malaria resulting from PbA infection, suggesting that the effector function of CD8$^+$ T cells is involved in the pathogenesis (9). However, it is unclear whether *Plasmodium*-specific CD8$^+$ T cells are activated during the erythrocyte stage of malaria and how they are involved in the pathogenesis of cerebral malaria.

Because malaria parasites infect RBC that do not themselves express MHC molecules, the infected cells cannot directly present malaria Ags to T cells in association with MHC class I molecules. To activate specific CD8$^+$ T cells, malaria Ags must be presented by a process referred to as cross-presentation by APCs that are themselves not infected, as reported for some minor histocompatibility Ags, tumor Ags, and various pathogens (12, 13). There are two main Ag presentation pathways of cross-presentation; one is the phagosome-to-cytosol pathway that is dependent on the TAP molecule (14), and the other is the TAP-independent pathway in which antigenic peptide is generated and loaded to MHC class I in MHC class II compartments (15) or on the cell surface by peptide regurgitation (16). The former TAP-dependent pathway is used by viruses that do not themselves infect hemopoietic cells (17) or some of the intracellular parasites such as *Mycobacterium tuberculosis* and *Toxoplasma gondii* (18, 19). The latter TAP-independent pathway is used by some pathogen-derived Ags such as those from *Leishmania major* and virus-like particles (20, 21). It is unclear how these different pathways are selected in targeting the exogenous Ags to the MHC class I presentation pathway by each microbial species.

Because class I-restricted Ags have not been identified in malaria parasites during the erythrocyte stage, we used a model Ag OVA to study immune responses of Ag-specific CD8$^+$ T cells

*Division of Immunology, Department of Molecular Microbiology and Immunology, and †Atomic Bomb Disease Institute, Graduate School of Biomedical Sciences, Nagasaki University, Nagasaki, Japan; and ‡Department of Medical Zoology, School of Medicine, Mie University, Tsu, Japan

Received for publication October 19, 2007. Accepted for publication May 13, 2008.

The costs of publication of this article were defrayed in part by the payment of page charges. This article must therefore be hereby marked *advertisement* in accordance with 18 U.S.C. Section 1734 solely to indicate this fact.

[1] This work was supported by Grants-in-Aid from the Ministry of Education, Science, Sports and Culture, Japan; and by the 21c COE program at Nagasaki University.

[2] Address correspondence and reprint requests to Dr. Katsuyuki Yui, Division of Immunology, Department of Molecular Microbiology and Immunology, Graduate School of Biomedical Sciences, Nagasaki University, 1-12-4, Sakamoto, Nagasaki, 852-8523 Japan. E-mail address: katsu@nagasaki-u.ac.jp

[3] Abbreviations used in this paper: PbA, *Plasmodium berghei* ANKA; OVA-PbA, recombinant *Plasmodium berghei* ANKA expressing OVA; WT-PbA, wild-type *Plasmodium berghei* ANKA; hsp, heat shock protein; DHFR-ts, dihydrofolate reductase-thymidyltransferase-ts; KO, knockout; LCMV, lymphocytic choriomeningitis virus; DC, dendritic cell; CD62L, CD62 ligand; OVAp, $OVA_{257-264}$ peptide.

during malaria infection. We generated a recombinant PbA that expresses a cytoplasmic form of OVA (OVA-PbA). Using this system, we show that malaria Ags can be presented to specific $CD8^+$ T cells by cross-presentation in a TAP-dependent manner during the erythrocyte stage of malaria infection and that these activated $CD8^+$ T cells could be pathogenic to the host. Furthermore, $CD8^+$ T cells that are not specific for malaria Ag can be activated during malaria infection in an Ag-nonspecific manner. This activation was at least in part dependent upon the presence of NK cells.

Materials and Methods

Generation of recombinant PbA parasite clones expressing OVA

Recombinant PbA parasites were engineered to constitutively express a truncated C-terminal fragment of OVA (aa 150–386) fused to the N-terminal sequence (aa 1–5) of the PbA heat shock protein (hsp) 70 gene. The gene construct was based on pBluescript KS^+ (Stratagene) and contains the following elements: 1) PbA dihydrofolate reductase-thymidyltransferase-ts (DHFR-ts) gene; 2) PbA hsp70 5′-untranslated region and N-terminal coding sequence; 3) coding sequence of C-terminal fragment of OVA; 4) PbA hsp70 3′-untranslated region and DHFR-ts 3′-untranslated region. The DHFR-ts gene contains a point mutation at position 110 of the DHFR gene causing a Ser→Asn transition conferring resistance to the antimalaria drug pyrimethamine.

The procedure to generate recombinant PbA was described previously (22). In brief, the gene construct was digested with *Sac*I and *Kpn*I to linearize and release the insert from the vector. PbA merozoites were transfected by electroporation and were selected in rats using pyrimethamine. The surviving parasites were further selected by limiting dilution in mice, and parasite clones that were resistant to pyrimethamine were obtained.

Mice, adoptive transfer, and PbA infection

OT-I-transgenic mice expressing the TCR specific for $OVA_{257-264}/K^b$ (23), were provided by Dr. H. Kosaka (Osaka University, Osaka, Japan), TAP knockout (TAP-KO) mice (C57BL/6 (B6) background; Ref. 24) by Dr. H. Watanabe (University of the Ryukyus Okinawa, Japan), B6.SJL-Ptprc congenic (B6.SJL) mice ($CD45.1^+$) by Dr. Y. Takahama (University of Tokushima, Tokushima, Japan), and RAG2 knockout (RAG2-KO) mice (25) by Dr. Y. Yoshikai (Kyushu University, Fukuoka, Japan). TCR P14 lymphocytic choriomeningitis virus (LCMV)/TCRα-KO mice (26) were purchased from Taconic. B6 mice were purchased from SLC. OT-I and B6.SJL mice were bred, and offspring were intercrossed to obtain CD45.1 OT-I mice. RAG2-KO mice and OT-I mice were intercrossed to obtain RAG2-KO OT-I mice. These mice were maintained in the Laboratory Animal Center for Animal Research at Nagasaki University (Nagasaki, Japan) and were used at the age of 8–14 wk. For adoptive transfer, $CD8^+$ T cells (>95%) were purified from CD45.1 OT-I mice using anti-CD8 IMag (BD Biosciences), labeled with CFSE (15 μM; Molecular Probes) and were injected into the tail vein of B6 mice ($0.7–2 \times 10^7$/mice). Mice were infected with WT-PbA or OVA-PbA by i.p. injection of parasitized RBCs (10^4 infected RBC) or by i.v. injection of 10^6 parasitized RBC (Fig. 2*C*). Parasitemia was monitored by microscopic examination of standard blood films, and mice were sacrificed after the parasitemia reached 1.6–18.2% (days 7–9). Brain sequestered lymphocytes were prepared as described (27). Depletion of NK cells was performed by injection of anti-NK1.1 mAb (PK136; 50 μl of ascites fluid partially purified by ammonium sulfate precipitation method) i.p. at −1 day, and i.v. at 2, 5, and 7 days after infection with PbA. The animal experiments reported herein were approved by the Institutional Animal Care and Use Committee of Nagasaki University and were conducted according to the guidelines for Animal Experimentation at Nagasaki University.

Immunoblotting

Peripheral blood cells of PbA-infected mice were washed and then lysed in PBS by freezing and thawing. After centrifugation, lysate (10^7 RBC) was separated on 15% SDS-PAGE and transferred to polyvinylidene difluoride membrane. The blot was blocked and probed with rabbit anti-OVA (Bethyl Laboratories) or rabbit anti-merozoite surface protein 1 Ab. After a washing, the membrane was incubated with HRP-conjugated anti-rabbit Ig Ab, washed, and analyzed using ECL reagents.

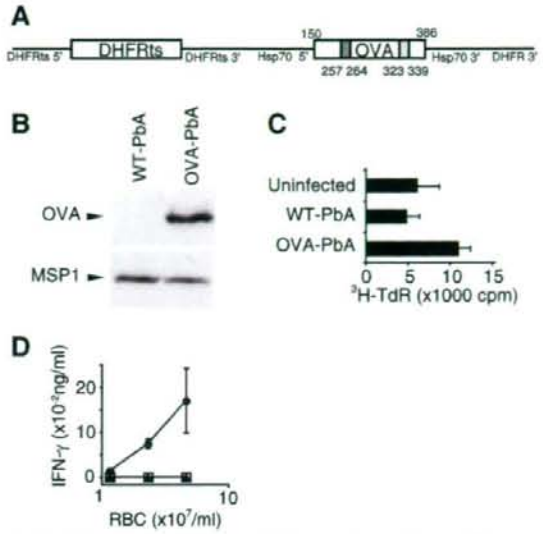

FIGURE 1. The expression of OVA in recombinant PbA. *A*, DNA construct to generate recombinant PbA. The C-terminal OVA coding sequence (aa 150–386) was fused to the N terminus (aa 1–5) of the PbA hsp70 gene. The expression of OVA was controlled by the PbA hsp70 promoter, which is constitutively active during liver and blood stages of the malaria life-cycle. DHFR-ts is a selection marker, which confers resistance to the antimalaria drug pyrimethamine. *B*, The lysates of RBC from B6 mice infected with WT-PbA or OVA-PbA were separated by SDS-PAGE, blotted, and probed with anti-OVA Ab and with anti-merozoite surface protein 1 Ab as control. *C*, OT-I T cells (3×10^5) and splenic DCs ($CD11c^+$ cells, 1×10^4) were cultured in the presence of uninfected freeze-thaw lysates of 9.3×10^6 RBCs or those infected with WT-PbA or OVA-PbA for 2 days, and pulsed for 20 h with [^{3}H]TdR. Parasitemia levels: WT-PbA, 16.9%; OVA-PbA, 18.4%. *D*, OT-I spleen cells (1×10^5) were cultured in the presence of DCs ($CD11c^+$ cells, 3×10^3) and RBCs from uninfected mice (□) or mice infected with WT-PbA (▲) or OVA-PbA (●) for 48 h. The production of IFN-γ in the supernatant was determined by ELISA.

Proliferation and IFN-γ production in vitro

To isolate dendritic cells (DC), B6 spleen was treated with dispase (5 μg/ml; Godo-shusei) for 30 min at 37°C. Spleen cells were treated with anti-CD11c microbeads, and DCs ($CD11c^+$, >90%) were purified using Auto MACS (Miltenyi Biotech). Proliferation of OT-I was determined by culture of OT-I $CD8^+$ T cells (1×10^5) in the presence of DC (3×10^3) and crude RBC Ag (9.3×10^6 RBCs) for 63 h with [^{3}H]TdR for the final 15 h. For IFN-γ assay, OT-I $CD8^+$ T cells (3×10^5) were stimulated with DCs (1×10^4) in the presence of crude malaria Ag (9.3×10^6 RBC) for 48 h, and the levels of IFN-γ in the supernatant were determined by a sandwich ELISA as described previously (28).

Flow cytometry

FcR was blocked with anti-FcγRII/III mAb (BD Biosciences). The staining reagents used in this study include PE-Cy7-anti-CD45.1, allophycocyanin- or PE-anti-CD8, FITC-anti-Vα2, PE- or FITC-anti-CD62 ligand (CD62L), FITC- or biotin-anti-CD44, and PE- or FITC-anti-CD69 mAbs (eBiosciences). $OVA_{257-264}$ H-$2K^b$ tetramer was purchased from MBL. 7-Aminoactinomycin D was added to exclude dead cells from the analysis. For analysis of granzyme B expression, splenocytes were incubated with Fc block and were stained with PE-Cy7-anti-CD45.1 and FITC- or allophycocyanin-anti-CD8 mAbs. Samples were fixed and permeabilized using Cytofix-Cytoperm buffer (BD Biosciences), stained with PE-anti-granzyme B mAb (Caltag), and analyzed using FACSCanto II (BD Biosciences).

Cytotoxicity assay in vitro and in vivo

For in vitro cytotoxicity assay, $CD8^+$ T cells were enriched from spleen cells by $CD8a^+$ T cell isolation kit (Miltenyi Biotech). EL4 target cells

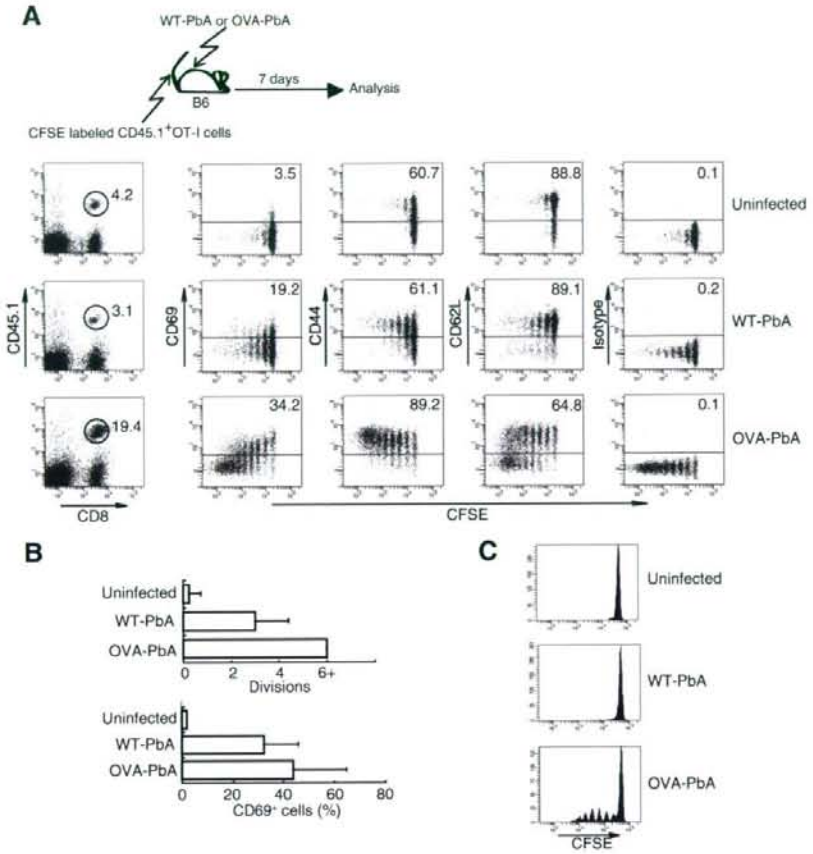

FIGURE 2. Ag-specific and -nonspecific activation of OT-I CD8$^+$ T cells in vivo during PbA infection. *A*, CFSE-labeled OT-I CD8$^+$ T cells (CD45.1$^+$, 8.8×10^6) were adoptively transferred into B6 mice, and the mice were uninfected or infected with WT-PbA or OVA-PbA (1×10^4) i.p. on the same day. Seven days later, spleen cells were stained with allophycocyanin-anti-CD8, PE-Cy7-anti-CD45.1, and PE-anti-activation markers (CD69, CD44, CD62L). Staining profiles of activation markers and CFSE are shown for the CD45.1$^+$CD8$^+$ gated population. Numbers in the upper right corner indicate percent of cells above the line. Levels of parasitemia: WT-PbA, 10.0%; OVA-PbA, 8.4%. *B*, Summary of cell divisions in the spleen after adoptive transfer of CFSE-CD8$^+$ T cells (*top*). Data were obtained from four independent experiments similar to *A*. *Bottom*, Percentage of CD69$^+$CD8$^+$ T cells obtained from six independent experiments similar to *A* except that transferred OT-I cells were not labeled with CFSE and the staining was performed using FITC-anti-CD69 mAb. In both panels, three groups showed a significant difference in overall comparison ($p < 0.05$; *top*, Savage test; *bottom*, Kruskal-Wallis test); each bar and whisker denote the mean and SD, respectively. The difference in the number of cell divisions was slightly not significant between uninfected and WT-PbA-infected mice ($p = 0.0187$, Savage test), whereas it was significant between uninfected and OVA-PbA-infected mice ($p = 0.0046$), and between WT-PbA-infected and OVA-PbA-infected mice ($p = 0.0047$). The proportion of CD69$^+$CD8$^+$ T cells was significantly higher in WT-PbA-infected ($p = 0.0025$, Wilcoxon rank-sum test) and OVA-PbA-infected mice ($p = 0.0025$) when compared with uninfected mice, whereas it was not significant ($p = 0.1490$) between WT-PbA-infected and OVA-PbA-infected mice. *C*, CFSE-labeled OT-I CD8$^+$ T cells (CD45.1$^+$, 1×10^7) were adoptively transferred into B6 mice, which were uninfected or infected with the large dose (1×10^6) of WT-PbA or OVA-PbA i.v. Three days later, spleen cells were analyzed using flow cytometry. Levels of parasitemia: WT-PbA, 1.3%; OVA-PbA, 1.0%.

were labeled with ^{51}Cr with and without $OVA_{257-264}$ peptide (OVAp) for 1 h at 37°C. Target and effector cells were added to each well of a 96-well plate and cultured for 4 h. Percent specific lysis = [(experimental ^{51}Cr release − spontaneous ^{51}Cr release)/(maximum ^{51}Cr release − spontaneous ^{51}Cr release)] × 100. For in vivo cytotoxicity assay, B6 spleen cells were labeled with a high concentration of CFSE (10 μM) and were pulsed with OVAp (1 μg/ml) for 1 h at 37°C or labeled with low concentration of CFSE (1 μM) and were incubated without peptide. Cells from each population were mixed at a 1:1 ratio, and a total of 1×10^7 cells were adoptively transferred into the recipient mice. Mice were sacrificed 4 h later, and spleen cells were analyzed using flow cytometry. Percent specific lysis = [1 − (ratio of peptide-pulsed cells)/(ratio of peptide-unpulsed cells)] × 100.

Evaluation of the disease

Mice were monitored daily after day 5 of infection, and clinical scores were defined by the presence of the typical pathological signs as described (29): level 1, hunching or wobbly; level 2, hunching and wobbly; level 3, hypotonia; level 4, limb paralysis and convulsions; level 5, death.

Statistical analysis

In comparison of three or more groups, overall comparison was first made by ANOVA for one-way or two-way data at the significance level of 0.05, and if significant, each pair of the groups was compared by *t* test. If the ordinary ANOVA was considered to be inappropriate because of the significant departure from normality, censoring in measurements or large variation in the variance among groups, the Kruskal-Wallis test, the Wilcoxon rank-sum test, or the Savage test was used instead with the significance level determined by the Bonferroni procedure controlling the familywise error rate <0.05. For survival data, the log-rank test was used in a similar way. Procedures of ANOVA, LIFETEST, and NPAR1WAY in the SAS system were used for the calculations.

Results

Ag-specific and nonspecific activation of CD8$^+$ T cells during PbA infection

We generated recombinant malaria PbA parasite that constitutively expresses the C-terminal fragment of OVA (aa 150–386) fused to the N terminus of PbA hsp70 (OVA-PbA; Fig. 1*A*). The expression of the recombinant OVA was confirmed by immunoblotting of the infected RBC lysates with anti-OVA Ab (Fig. 1*B*). The ability of DCs to present OVA-PbA Ag was evaluated for proliferation and IFN-γ secretion of OVA-specific OT-I CD8$^+$ T cells in vitro (Fig. 1, *C* and *D*). CD8$^+$ T cells from OT-I mice showed specific proliferation and IFN-γ secretion in response to the DCs pulsed with OVA-PbA-infected RBC. We used adoptive transfer of OT-I CD8$^+$ T cells from TCR-transgenic mice to determine whether Ag-specific CD8$^+$ T cells can be primed during PbA infection. B6 mice (CD45.2$^+$) were adoptively transferred with CFSE-labeled OT-I CD8$^+$ T cells (CD45.1$^+$) and were infected with wild-type *P. berghei* ANKA (WT-PbA) or OVA-PbA. The proliferation of OT-I CD8$^+$ T cells was monitored by the sequential loss of CFSE intensity 7 days after infection (Fig. 2, *A* and *B*). The proportion of OT-I CD8$^+$ T cells increased in mice infected with OVA-PbA (19.4%) when compared with uninfected mice (4.2%) or mice infected with WT-PbA (3.1%). OT-I CD8$^+$ T cells divided minimally and remained CD69$^-$CD44^{low}CD62L^{high} in the uninfected host. Extensive division of OT-I CD8$^+$ T cells was observed in mice infected with OVA-PbA. In addition, up-regulation of the CD69 marker was observed in cells that divided 0–3 times, and up-regulation of CD44 and down-regulation of CD62L were evident in cells that have divided multiple times, indicating that OT-I CD8$^+$ T cells were activated in an Ag-specific manner during infection with PbA. Unexpectedly, OT-I CD8$^+$ T cells divided ~4 times and up-regulated the CD69 marker in mice infected with WT-PbA, suggesting that OT-I CD8$^+$ T cells can be activated in an Ag-nonspecific manner during infection with WT-PbA. Because it was recently reported that malaria infection impairs cross-presentation (30), we examined the ability of host APC to present OVA-PbA Ag during early (days 0–3) and late (days 5–8) periods after infection (Figs. 2*C* and 4*A*, *left*). In both periods, OT-I cells proliferated several times in vivo after infection with OVA-PbA but not with WT-PbA, indicating that APC can cross-present malaria Ag throughout infection with PbA.

We have also analyzed lymphocytes in the brain. The number of CD8$^+$ T cells retained within the brain was increased in mice infected with WT-PbA or OVA-PbA (Fig. 3*A*). A large variation in the number of CD8$^+$ T cells in the infected mice might reflect their differential stages of cerebral malaria. OT-I cells, however, were increased only in mice infected with OVA-PbA. The number of CD4$^+$ T cells was not significantly different between these groups of mice. We also examine the CFSE profile and surface phenotype of OT-I cells that were sequestered in the brain (Fig. 3*B*). OT-I cells in the brain of OVA-PbA-infected mice uniformly showed low levels of CFSE and CD44^{high}CD62L^{low} phenotype, indicating that only highly activated OT-I cells were retained within the brain of mice infected with OVA-PbA.

Activation of malaria-specific CD8$^+$ T cells is TAP dependent

To determine whether the Ag presentation of OVA epitope to OT-I CD8$^+$ T cells utilize the conventional class I Ag presentation pathway, we examined the requirement for the TAP molecule in proliferation of OT-I CD8$^+$ T cells in vivo in TAP null mice (TAP-KO; Fig. 4, *A* and *C*). In this experimental system, we monitored the T cell response in vivo within 3 days after transfer, given that the number of OT-I CD8$^+$ T cells was severely reduced 5 days after transfer, perhaps due to their rejection in TAP-KO host mice (data not shown). Thus, we infected B6 or TAP-KO mice with WT-PbA or OVA-PbA, adoptively transferred CFSE-labeled CD8$^+$ T cells from CD45.1$^+$OT-I mice 5 days later, and monitored proliferation of OT-I T cells by the sequential loss of CFSE intensity 3 days later (parasitemia 2.3–5.4%). Division of OT-I cells was not detectable in uninfected or WT-PbA-infected hosts during these 3 days. In B6 mice infected with OVA-PbA, however, OT-I cells divided several times, indicating that they were activated in vivo in an Ag-specific manner. In TAP-KO hosts, no proliferative responses were observed, indicating that Ag presentation of the OVA epitope expressed in OVA-PbA in association with the MHC class I molecule, was dependent on the TAP molecule. However, OT-I CD8$^+$ T cells showed increased expression of CD69 and reduced expression of CD62L in the TAP-KO host mice infected with WT-PbA or OVA-PbA, suggesting that these phenotypical changes of OT-I CD8$^+$ T

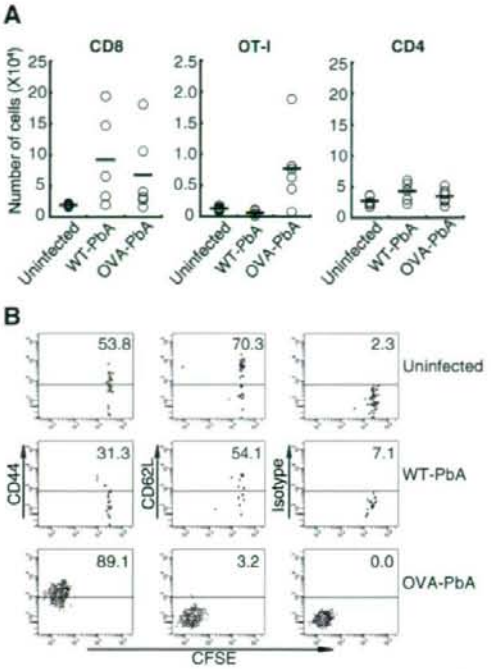

FIGURE 3. Sequestration of T cells in the brain of mice infected with PbA. *A*, B6 mice were adoptively transferred with OT-I CD8$^+$ T cells (CD45.1$^+$) and were uninfected or infected with WT-PbA or OVA-PbA. After elevation of parasitemia (WT-PbA, 2.2–12.9%; OVA-PbA, 1.2–8.4%), lymphocytes in the brain were collected and stained with allophycocyanin-anti-CD8, PE-anti-CD4, and PE-Cy7-anti-CD45.1 mAb. The numbers of T cell subsets were determined by multiplying the total number of cells with the percentage of each population. Overall comparison showed a significant difference both in the number of CD8$^+$ T cells and in OT-1 ($p < 0.05$, Kruskal-Wallis). However, the difference in the former was slightly not significant between uninfected and WT-PbA-infected mice ($p = 0.0179$, Wilcoxon rank-sum test) and between uninfected and OVA-PbA-infected mice ($p = 0.0328$), whereas in the latter the difference was significant between OVA-PbA-infected mice and WT-PbA-infected mice ($p = 0.0112$) and was slightly not significant between OVA-PbA-infected mice and uninfected mice ($p = 0.0328$). Overall comparison of the number of CD4 showed no significant difference ($p = 0.1394$, Kruskal-Wallis test). *B*, CFSE-labeled OT-I CD8$^+$ T cells (CD45.1$^+$) were adoptively transferred into B6 mice, which were uninfected or infected with WT- or OVA-PbA. Brain lymphocytes were stained with mAbs as described in Fig. 2*A*. Staining profiles of activation markers and CFSE are shown for the CD45.1$^+$CD8$^+$ gated populations. Numbers in the upper right corner indicate percentage of cells above the line. Levels of parasitemia: WT-PbA, 10.1%; OVA-PbA, 9.4%. Representative data of two similar results are shown.

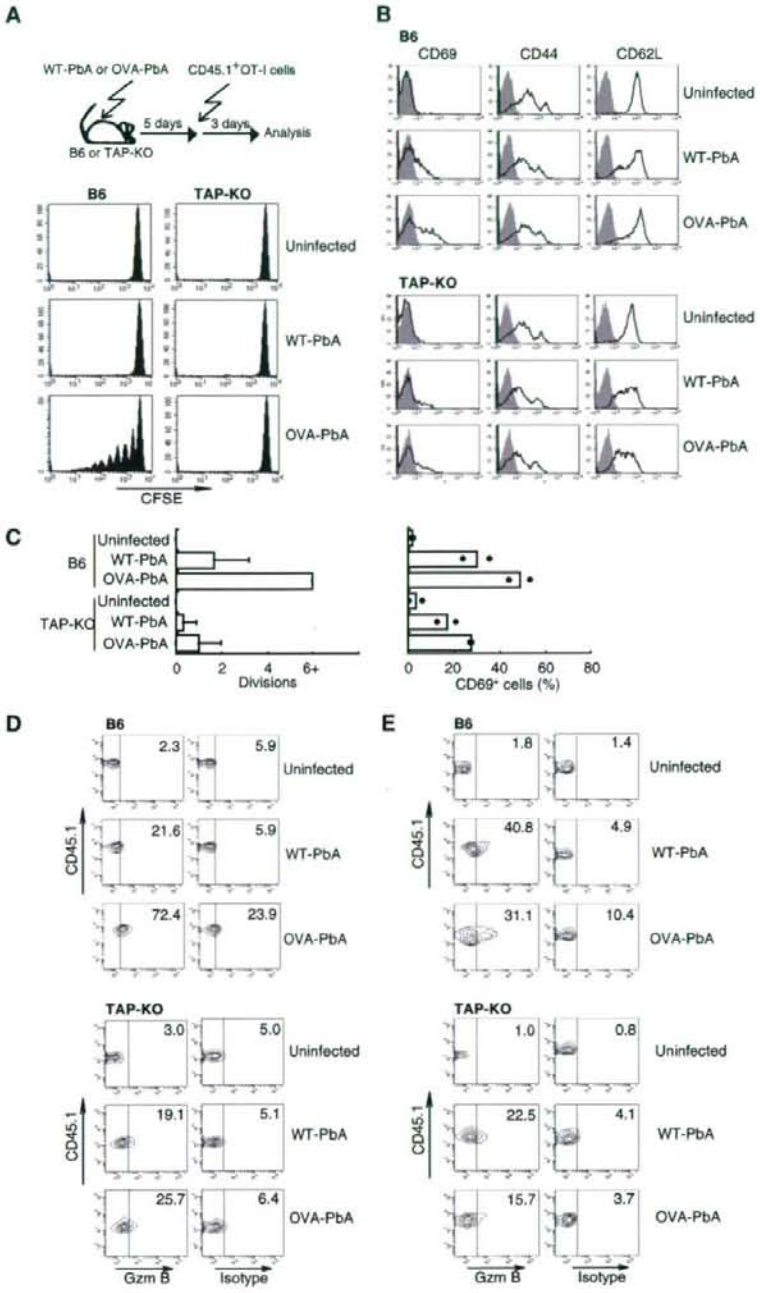

FIGURE 4. Specific activation of OT-I CD8+ T cells during infection with OVA-PbA is TAP dependent. B6 or TAP-KO mice were uninfected or infected with WT-PbA or OVA-PbA. Five days later, mice were inoculated with CFSE-labeled CD8+ T cells (1×10^7 in *A*, 2×10^7 in *B*) from CD45.1+OT-I mice. Three days later, spleen cells were stained with allophycocyanin-anti-CD8, with PE-Cy7-anti-CD45.1 (*A*), or with additional FITC-antiactivation marker mAbs (CD69, CD44, CD62L) (*B*). The CFSE profiles (*A*) or staining profiles of activation markers (solid line) and isotype control (dark histogram) (*B*) of the CD45.1+CD8+ gated populations are shown. *C*, Summary of the cell divisions ($n = 3$) and CD69+ cells ($n = 2$; each dot represents the result of one mouse) performed as in *A* and *B*. In B6 mice, a significant difference was observed in overall comparison of the number of cell divisions among three groups of mice ($p < 0.05$, Savage test), whereas no such difference was observed in TAP-KO mice. In B6 mice, the number of cell division was significantly larger in OVA-PbA-infected mice compared with WT-PbA-infected mice ($p = 0.0143$, Savage test) and uninfected mice ($p = 0.0127$), while the difference was not significant between WT-PbA-infected and uninfected ($p = 0.0732$); each bar and whisker denote the mean and SD, respectively. *D* and *E*, Staining profiles of the CD45.1+CD8+ gated populations of spleen cells prepared as in *B*, stained with allophycocyanin-anti-CD8, PE-Cy7-anti-CD45.1, and PE-anti-granzyme B (Gzm B) mAbs or PE-isotype control ex vivo before (*D*) and after culture on plates coated with anti-TCR mAb for 5 h (*E*). The number in each panel indicates the percentage of positive cells. The high background of the isotype control (23.9%) was observed without PE-isotype Ab, suggesting that it was due to autofluorescence. Levels of parasitemia in WT-PbA (3.2–5.4%) and OVA-PbA (2.4–6.1%)-infected B6 mice: WT-PbA (2.3–6.2%)-infected mice; and OVA-PbA (4.7–5.5%)-infected TAP-KO mice.

cells could be induced without TCR occupancy during PbA infection (Fig. 4, *B* and *C*). We also evaluated their expression of granzyme B by intracellular staining in this model. The expression of granzyme B was undetectable in OT-I CD8+ T cells in uninfected mice but was detected in OT-I CD8+ T cells in WT-PbA or OVA-PbA-infected mice both before and after culture (Fig. 4, *D* and *E*). The level of granzyme B expression in OT-I CD8+ T cells ex vivo was higher in OVA-PbA-infected mice than in WT-PbA-infected mice. OT-I CD8+ T cells transferred into TAP-KO mice also showed up-regulation of granzyme B expression, suggesting that it could be induced without TCR occupancy during malaria infection.

Involvement of NK cells in nonspecific activation of CD8+ T cells

It has been reported that NK cells are activated during malaria infection and play pivotal roles in the induction and recruitment of specific CD8+ T cells (31–33). To examine whether CD4+ T